Eidgenössische Technische Hochschule Zürich
Swiss Federal Institute of Technology Zurich

Power Electronic Systems Laboratory

Ismail Tezol

High-Speed Sensorless Motor Control with Improved Power Electronics Topologies

Master Thesis

Power Electronic Systems Laboratory (PES)
Swiss Federal Institute of Technology (ETH) Zurich

Supervision

M.Sc. Simon Nussbaumer
M.Sc. Michael Antivachis
Prof. Dr. Johann W. Kolar

August 2018

Celeroton AG
Industriestrasse 22
8604 Volketswil
Schweiz

Aufgabenstellung

Art:	Masterarbeit
Studenten:	Ismail Tezol
Nummer:	SAC1801 (PES-Nummer: LEM1803)
Datum:	19.02.2018-17.08.2018
Betreuer Celeroton:	Simon Nussbaumer
Betreuer ETH:	Michael Antivachis
Professor:	Prof. Dr. Johann W. Kolar
Titel:	High-Speed Sensorless Motor Control with Improved Power Electronics Topologies

Inhaltsverzeichnis

1 Einführung

An der Professur für Leistungselektronik werden neue Topologien und Modulationsverfahren für ultra-high-speed-Motoren entwickelt. Diese Motoren benötigen verbesserte sensorlose Regelungsverfahren, da herkömmliche Methoden, basierend auf einer Messung der Nulldurchgänge der Gegenspannung nicht mehr anwendbar sind. Deshalb soll in dieser Arbeit ein Positionsschätzer (Observer) für diese Topologien entwickelt werden. Dies beinhaltet die Weiterentwicklung von bekannten Observern für den Einsatz mit AC Filtern, hochfrequenten Motorströmen und hohen Inverterschaltfrequenzen. Der Observer soll auf Messungen der Motorströme und Motorspannungen, sowie auf einem Motormodell basieren. Das Blockschaltbild der Drehzahlregelung inklusive des zu implementierenden Observer ist in Abbildung 1 dargestellt.

In einem ersten Schritt soll der Observer entwickelt und mit Hilfe einer Simulation verifiziert werden. Der Observer soll für verschieden Umrichtertopologien und Modulationsverfahren entwickelt werden. In einem zweiten Schritt soll der Observer auf einer Kontroll-Platform(DSP/FPGA) implementiert werden und in zwei verschiedenen Umrichtern getestet werden. Abschliessend sollen zusammen mit einem High-Speed Motor Messungen bei verschiedenen Drehzahlen, sowie bei Drehzahlsprüngen durchgeführt werden.

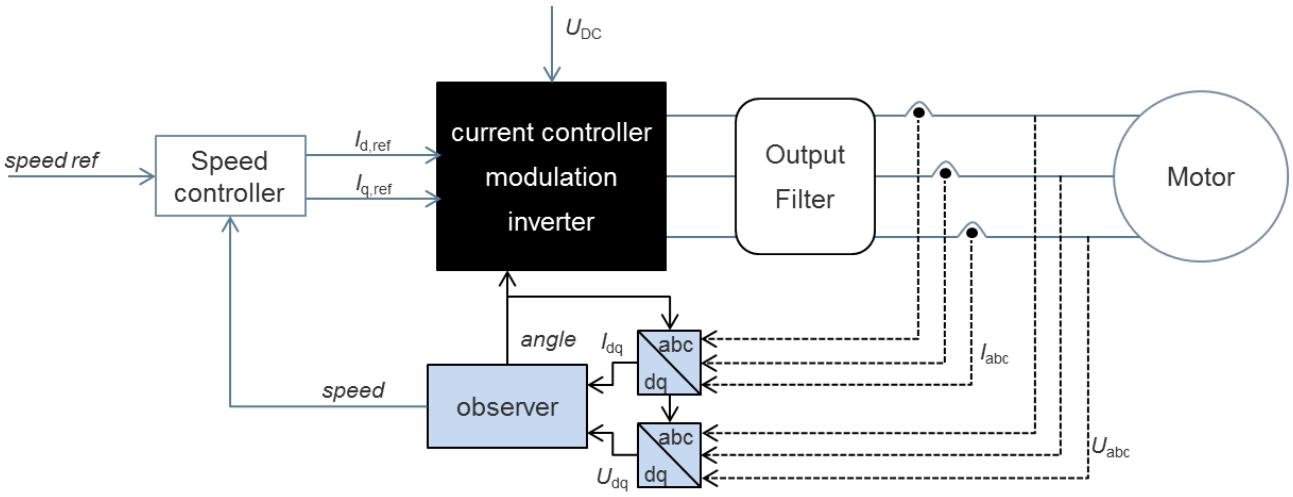

Abbildung 1:Blockschaltbild der Drehzahlregelung (inkl. Observer)

2 Aufgabenstellung

2.1 Einstiegsaufgabe

2.1.1 Inbetriebnahme des Umrichters DC1

Am Anfang der Arbeit soll der Umrichter DC1 zusammen mit einem Testmotor ohne Observer in Betrieb genommen werden, wobei eine bestehende Winkelsensorik zur Verfügung steht. . Auf diesem Umrichter sollspäter der Winkel-Observer implementiert werden. Dazu gehören folgende Arbeitsschritte:

- Verkabelung des Umrichters/Motors
- Laden der Firmware
- Betrieb des Motors bei verschiedenen Drehzahlen/Control Modes

In einem zweiten Schritt soll die CPU Auslastung bei verschiedenen Betriebspunkten gemessen werden. Diese Messungen geben Aufschluss darüber, ob noch genügend Rechenkapazität für die Observer Implementation zur Verfügung steht, oder ob die Firmware des DC1 noch optimiert werden muss.

2.1.2 Literaturstudium

Parallel zu der praktischen Einstiegsaufgabe soll die Literatur gemäss Kapitel 4 studiert werden. Im Rahmen dieses Literaturstudium sollen verschiedene Observer-Konzepte evaluiert werden.

2.2 Simulation verschiedener Observer-Konzepte

Die im Literaturstudium evaluierten Observer-Konzepte sollen mit Hilfe von Matlab/SIMULINK simuliert und miteinander verglichen werden. In einem ersten Schritt werden für die Simulation sinusförmigen Ströme und Spannungen angenommen. In einem zweiten Schritt soll die Strom- und Spannungsverläufe der verwendeten Umrichter (DC1 und DC2) verwendet werden. Die Strom- und Spannungsverläufe der Umrichter sollen mittels einer Simulation in Gecko ermittelt werden.

Die verschiedenen Observer-Konzepte sollen anhand der Simulation und des Literaturstudiums miteinander verglichen werden. Dabei sollen folgende Kriterien untersucht werden:

- Genauigkeit der Winkelschätzung
- Einfluss von Störungen der Strom/Spannungsmessung
- Rechenaufwand

2.3 Implementierung des Observers

Anhand der Simulationsergebnisse sollen ein bis zwei Observer-Konzept ausgewählt und auf dem Umrichter DC1 implementiert werden. Dazu soll für die Regelung weiterhin die Winkelmessung der Winkelsensorik verwendet werden und parallel dazu über den Observer den Winkel geschätzt werden. Der geschätzte Winkel des Observers soll mit der Winkelmessung unter verschieden Bedingungen verglichen werden:

- Bei unterschiedlichen Drehzahlen
- Im Leerlauf/unter Last
- Bei einem Drehzahlsprung
- Bei einem Lastsprung

Die Messungen sollen mit den Resultaten der Simulation verglichen werden.

2.4 Regelung unter Verwendung der Winkelschätzung des Observers

Die Firmware des DC 1 soll so angepasst werden, dass die Winkelschätzung des implementierten Observers für die Regelung der Phasenströme und der Drehzahl verwendet wird.

Anschliessend soll mittels Messungen die Performance gegenüber der Regelung mit der Winkel Sensorik verglichen werden. Folgende Grössen sollen miteinander verglichen werden:

- Drehzahlstabilität
- Strom und Spannungsverläufe
- Leistungsaufnahme
- CPU Auslastung

2.5 Portierung auf den Umrichter DC2

Die Observer-Implementation soll auf den Umrichter DC2 portiert werden und die Messungen des der Kapitel 2.3 und 2.4 wiederholt werden.

3 Zeitplan

In den ersten 2 Wochen soll selbständig ein Zeitplan (nach Vorlage) für den Ablauf der Arbeit erstellt werden.

4 Literatur

[1] Roman Bosshard, Parameter Estimation and Sensorless Control of an Ultra-High-Speed PMSM, Masterarbeit, ETH Zürich, Zürich, Schweiz, 2011
[2] Observer für PWM Antrieb, Celerotoninternes Manual
[3] Hinweise für die Erstellung von Berichten – Celerotoninternes Manual

5 Dokumentation

Sämtliche wissenschaftlich relevanten Ergebnisse sind in einem Bericht schriftlich festzuhalten. Zusätzlich sollen die erstellte Firmware und Software auskommentiert und/oder dokumentiert sein, damit eine nahtlose Übergabe und Weiterarbeit garantiert werden kann. Die Dokumentation soll die Reproduzierbarkeit der Testumgebung gewährleisten und eine einfache Bedienungsanleitung beinhalten.

Hilfestellung zur Erstellung einer technischen Dokumentation gibt das Dokument „SOP-0005-Rev01 Celeroton Hinweise für die Erstellung von Berichten“. Die Dokumentation soll zudem nach den PES-Vorschriften in “Printing instruction Study- and Masterthesis PES” erstellt und gedruckt werden, wobei der Celeroton-interne Betreuer ebenfalls ein Exemplar erhalten soll. Zudem sollen die Geheimhaltungshinweise in Celerotons „Vereinbarung für Master-, Studien- und Gruppenarbeitsstudenten/innen“ beachtet werden.

6 Präsentation

Am Schluss der Arbeit soll das Erreichte in einem Vortrag von ca. 20 Minuten (plus 10 Minuten Fragen) präsentiert werden, einmal bei Celeroton und einmal an der ETH am PES. In der Mitte der Masterarbeit findet zudem eine Zwischenpräsentation bei Celeroton statt.

7 Allgemeine Hinweise

Folgende, beiliegende Dokumente sind integraler Bestandteil dieser Aufgabenstellung und müssen durchgelesen und unterschrieben werden:

- “Vorschriften über die Durchführung von EXTERNEN Studien- und Masterarbeiten” des PES/ETH
- „Vereinbarung für Master-, Studien- und Gruppenarbeitsstudenten/innen“ der Celeroton AG
- „Merkblatt für Studierende zum Thema Plagiate“ der ETH
- „Sicherheitsvorschriften“ der Celeroton AG“

Preface

This master thesis was written in summer 2018 at the spin-off company Celeroton in collaboration with the Power Electronics System Laboratory (PES) of the Swiss federal Institute of Technology in Zurich (ETH).

This master thesis provides a big challenge for sensorless motor control for ultra-high-speed range. It was very exciting to run the motor at high speed. This thesis is well rounded and has contributed a lot to my experience and knowledge. Therefore, I would like to thank my both supervisor Simon Nussbaumer and Michael Antivachis for their contribution in my thesis. Special thanks also to Christof Zwyssig and Celeroton AG family for the opportunity to write my thesis in Celeroton AG and their valuable contribution.
Zurich, August 2018

Ismail Tezol

Abstract

In Power Electronic System Laboratory and Celeroton AG new topologies and modulation technique have been developed for ultra-high-speed range drive systems. This drive systems require improved motor control techniques. A sensorless motor control is required to design and implement for the project of collaboration between PES and Celeroton AG up to 350 *krpm*. Therefore, different type of Observers, which estimate the speed and position of the rotor, is evaluated. Among different observer type, the Phase Locke Loop (PLL) Observer is selected. Two type of the PLL-Observer are examined, and design rules are determined. The PLL-Observer is modeled in an existing simulation environment and tested for verification the entire system. Finally, the PLL-Observer is implemented on two different controller board and tested for different operating points with a voltage source inverter and permanent magnet synchronous machine. The tests are made with a speed up to 170 *krpm* successfully.

Nomenclature

Symbols

f	frequency
$i, \boldsymbol{i}$	current, space vector
I	DC current
j	complex unit, $\sqrt{-1}$
n	speed, indices, noise
P	power
p	pole pair number
R	resistance
s	variable of the Laplace transformation
T	torque
$v, \boldsymbol{v}$	voltage, space vector
U	DC voltage
$\boldsymbol{x}$	state vector
δ	parameter error value
ψ	permanent-magnet flux
ϕ	back-EMF
ρ	observer bandwidth
ω	angular frequency
θ	rotor position
ε	error quantity
Dc	damping factor
K	application specific gain parameter

Indicies

a, b, c	phase a, b, c component
add	additional
c	cut-off frequency
d	direct-axis component
el	electrical
$exec$	execution
$filt$	speed filter
int	interrupt

L	inductive
$load$	load
$mech$	mechanical
N	nominal value
obs	observer
ph	phase component
pk	peak value
pm	permanent-magnet
q	quadrature-axis component
s	stator
$switch$	switching
tot	total
α	α-axis component
β	β-axis component
λ	speed limit
r	rotor
i	integral
p	proportional
∞	asymptotic
o	open loop
c	closed loop

Notation

$\hat{.}$	estimated value
$.^{\circ}$	electrical degree

Acronyms and Abbreviations

AC	alternating current
DC	direct current
DSP	digital signal processor
EKF	extended Kalman filter
EMF	electromotive force
ETH	Eidgenössische Technische Hochschule
FFT	fast Fourier transform
LO	Louenberg observer
MRAS	model reference adaptive system
PCB	printed circuit board
PES	Power Electronic Systems Laboratory
PLL	phase-locked loop
PMSM	permanent-magnet synchronous machine
PWM	pulse width modulation

Contents

Chapter 1

Introduction

The permanent magnet synchronous machine (PMSM) has been widely used in the industrial field. Especially, PMSM are used as variable speed applications in automobile, aerospace, health and micro machine areas. This kind of electrical machines shows high power density, reliability and robustness. A challenge of PMSM occurs in ultra-high-speed range, which needs special design requirements in field of mechanic, electronic and control. Therefore, Celeroton AG and PES-Laboratory collaborates to provide an ultra-high-speed drive system, which is enhanced with PMSM and improved inverter topologies.

The high-tech company Celeroton AG develops and provides ultra-high-speed drive system with commercial success. In this ultra-high-speed drive systems consist of low voltage inverters and permanent magnet synchronous machine (PMSM), which is special designed and optimized for high speed range. According to fundamental scaling law of mechanics, the motor can be designed smaller and compacter with increasing the rotational speed. The design of a such motor for high speed range is a big challenge. Therefore, the Celeroton AG has built a two-pole slot-less PMSM, which shows high mechanical rigidity. The built machine is a BackToBack (B2B) machine, which has two different windings around the rotor. One winding is used as a motor and the other winding as generator. This motor exhibits low leakage inductance. This can cause high current ripple and with reduction of the motor size, the loss density is increasing. The dissipation of the motor losses is difficult. Therefore, an electronic for the B2B machine must be designed to provide high quality phase currents.

In PES-Laboratory an inverter is designed to meet the requirements of the B2B machine. The chosen topology for the inverter is a Voltage Source Inverter (VSI). This inverter has an input voltage of 48 V and a rated power of 500 W. With a two-stage output filter, at the output of the inverter is provided high quality sinusoidal currents. With the collaboration of Celeroton AG, new generation inverter topologies are researched to provide higher power density and efficiency.

Another challenge within the project of the collaboration between PES-Laboratory and Celeroton AG is designing a controller for ultra-high-speed range. A common approach is a cascaded controller, which has an inner fast current controller and outer slow speed controller. The current controller performs in dq-Coordinate system, which depended on the rotor position. Therefore, position sensor is built for ultra-high-speed motors at Celeroton AG. However, Celeroton AG investigates on sensorless motor control technique to replace the position sensor with an Observer, which estimates the speed and position of the rotor. Therefore, within project of

the collaboration of PES-Laboratory and Celeroton AG, a design and implementation of an Observer on the controller board of VSI is a target. With designing and implementation of an observer, the electronic part of the ultra-high-speed drive systems are reduced regarding the volume. Therefore, an integrated inverter B2B machine can be provide.

An observer design for ultra-high-speed drive systems is another challenge. Especially the entire system of the project must be considered to design an appropriate observer, which can estimate the speed and position of the rotor in high speed range to run the system properly, because a model-based observer is depended on the machine (B2B) parameter and the output voltages anc currents of the inverter (VSI). At the same time, the implementation of the observer on a DSP with enough execution time is another limit.

With achieving the observer design for B2B, the position sensor will be not used anymore. The cost of the position sensor and physical volume are eliminated. This will provide more robust and rigid product. However, there are challenges of development of position and speed observer:

- A appropriate observer selection for ultra-high-speed range
- Limited computation time on DSP
- Satisfy the bandwidth requirement of the machine dynamics
- Start-up strategy to run the motor with a observer

The outline of this thesis is organized in the following chapters:

Machine and Inverter Model: In this chapter a simplified PMSM and VSI is derived. The derivation of the speed and current controller gain parameters are examined. The parameters of the Observer plant are based on this chapter.

Sensorless Motor Control: In this chapter, a selection criteria of different type observers are determined. Different observer types are examined and possible observer types are listed. The chosen Phase Locked Loop is presented in detail and design requirements are defined.

Simulation Setup and Results: Observer model is built and simulated for verification for a stable system. The simulation results are presented.

Hardware Setup and Results: Observer is implemented and tested for different working points. The Hardware results are presented.

Conclusion: A summary is made of the thesis and some suggestions are made for the future work.

Chapter 2

Machine and Inverter Model

In this chapter, a theoretical foundation of the B2B-Motor (PMSM) and the VSI topology are presented. Furthermore, the derivation of the current and speed controller is explained. The theories and equations of this chapter will form the basis of designing an Observer for the B2B machine.

2.1 Electrical equations of the PMSM

PMSM is in the AC motor category, which is referred to alternative currents to feed the motor. In this situation 3-Phase sinusoidal current is put on the motor terminal to run the motor synchronously with the phase current frequency. 3-Phase motors equations can be described in three ways [1] (Figure 2.1):

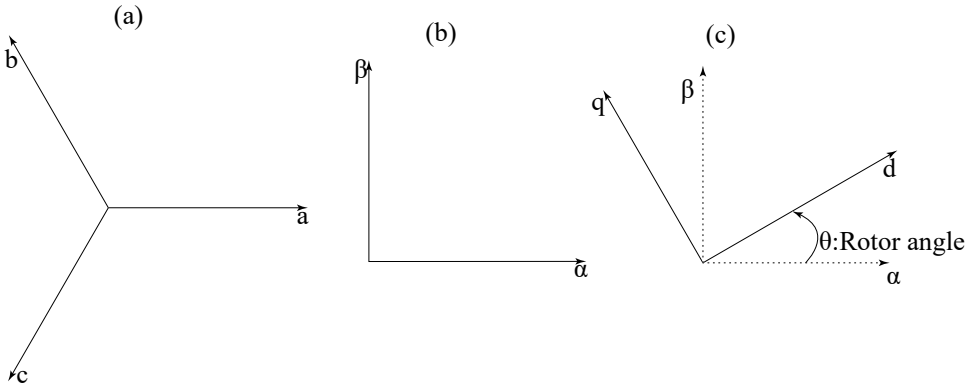

Figure 2.1: Different coordinate systems: a) *abc*-frame b)$\alpha\beta$-frame c)*dq*-frame

- *abc*-frame: Fixed three axis frame
- $\alpha\beta$-frame: Fixed two axis frame
- *dq*-frame: Rotational two axis frame

abc-frame is refereed to three phases stationary refences. This frame represents the physical reference frame of the motor. Current and voltage measurements of the inverter are made in this frame and axis of the frame is fixed.

Electrical equations of the PMSM at *abc* frame is given below:

$$\begin{pmatrix} v_{s,a} \\ v_{s,b} \\ v_{s,c} \end{pmatrix} = R_s \begin{pmatrix} i_{s,a} \\ i_{s,b} \\ i_{s,c} \end{pmatrix} + L * \frac{d}{dt} \begin{pmatrix} i_{s,a} \\ i_{s,b} \\ i_{s,c} \end{pmatrix} + \omega_{el} \frac{d}{dt} \begin{pmatrix} \psi_{s,a} \\ \psi_{s,b} \\ \psi_{s,c} \end{pmatrix} \tag{2.1}$$

where v_{sabc} is the stator phase voltages, R_s is the stator winding resistance, i_{sabc} is the stator phase currents and ψ_{rabc} is the magnet flux of the rotor, which is induced by the permanent magnet. L is the stator inductance matrix. The last components represents the back electromotive force (back-EMF), which is induced by the rotor:

$$\begin{pmatrix} \phi_{s,a} \\ \phi_{s,b} \\ \phi_{s,c} \end{pmatrix} = \omega_{el} \frac{d}{dt} \begin{pmatrix} \psi_{s,a} \\ \psi_{s,b} \\ \psi_{s,c} \end{pmatrix} \tag{2.2}$$

For speed and current control of the motor and inverter, the *abc* phase currents needs to be transformed onto rotating two phase coordinates, which is refereed as Park Transformations. This is made in two steps. First, three phase stationary *abc*-frame is transformed with Clark transformations onto the two-phase stationary $\alpha\beta$-frame, which is defined in equation 2.3.

$$\begin{pmatrix} x_\alpha \\ x_\beta \end{pmatrix} = \sqrt{\frac{2}{3}} \begin{pmatrix} 1 & -\frac{1}{2} & -\frac{1}{2} \\ 0 & \frac{\sqrt{3}}{2} & -\frac{\sqrt{3}}{2} \end{pmatrix} \begin{pmatrix} x_a \\ x_b \\ x_c \end{pmatrix} \tag{2.3}$$

With the equation 2.1 and 2.3 the voltage equation of the PMSM is obtained in $\alpha\beta$ frame as

$$\begin{pmatrix} v_\alpha \\ v_\beta \end{pmatrix} = L_{s_{d,q}} \frac{d}{dt} \begin{pmatrix} i_\alpha \\ i_\beta \end{pmatrix} + R_s \begin{pmatrix} i_\alpha \\ i_\beta \end{pmatrix} + \begin{pmatrix} \phi_\alpha \\ \phi_\beta \end{pmatrix} \tag{2.4}$$

where $L_{s_{d,q}}$ is the stator inductance in dq frame. The back-EMF equations are given as:

$$\begin{pmatrix} \phi_\alpha \\ \phi_\beta \end{pmatrix} = \sqrt{\frac{3}{2}} \psi_r \omega_{el} \begin{pmatrix} -sin(\theta_{el}) \\ cos(\theta_{el}) \end{pmatrix} \tag{2.5}$$

where θ_{el} is the electrical position of the rotor and is equal to the rotor mechanical position, because the pole pair number is $p = 1$ ($\theta_{el} = p\theta_r$, $\omega_{el} = p\theta_r$).

From stationary two phase rotating two phase frames is achieved. To obtain two phase rotating frame the equation 2.6 is used, which is dependent on the rotor position.

$$\begin{pmatrix} x_d \\ x_q \end{pmatrix} = \begin{pmatrix} sin(\theta_{el}) & cos(\theta_{el}) \\ cos(\theta_{el}) & -sin(\theta_{el}) \end{pmatrix} \begin{pmatrix} x_\alpha \\ x_\beta \end{pmatrix} \tag{2.6}$$

With the rotor angle θ_r the d axis of the frame is aligned with rotor flux ψ_r and q component of the current is vertical to the magnet flux. The voltage equation of the PSMSM is given as:

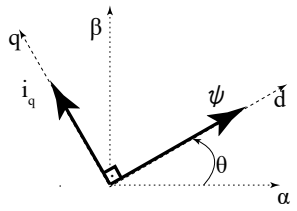

Figure 2.2: Magnet flux and q component of the current in dq-frame

$$\begin{pmatrix} v_d \\ v_q \end{pmatrix} = L_{s_{d,q}} \frac{d}{dt} \begin{pmatrix} i_d \\ i_q \end{pmatrix} + R_s \begin{pmatrix} i_d \\ i_q \end{pmatrix} + \begin{pmatrix} \phi_d \\ \phi_q \end{pmatrix} \tag{2.7}$$

The back-EMF equation then given as:

$$\begin{pmatrix} \phi_d \\ \phi_q \end{pmatrix} = \begin{pmatrix} -L_{s_{d,q}} i_q \omega_{el} \\ L_{s_{d,q}} i_d \omega_{el} + \psi_r \omega_{el} \end{pmatrix} \tag{2.8}$$

The electromagnetic torque is produced by q-component of the current, which is given in the equation 2.9 and the newton's law of motion, which describes the mechanical dynamics of the system is given in equation 2.10:

$$T_{em} = \frac{3}{2} \psi_r i_q \tag{2.9}$$

$$J \frac{d}{dt} \omega_r = T_{em} - f\omega_r - T_L \tag{2.10}$$

where J is the inertia of the rotor, f is the visous factor, T_L is the load torque.

2.2 Inverter Model

In this chapter the inverter model (VSI), which is used for the for high-speed motor, is explained.

2.2.1 Voltage Source Inverter

A voltage source inverter (VSI) is a frequency inverter structure, which is used in industry. In this thesis a direct VSI is used. The used VSI is made at ETHZ and will be shown in the Chapter 7. A scheme of the VSI with an output filter is shown in figure 2.3.

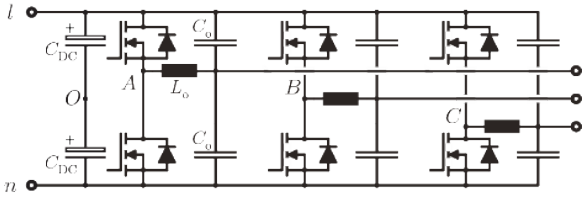

Figure 2.3: Voltage Source Inverter

The VSI consist of a DC-Link with full bridge rectifier. The DC-Link is coupled with a capacitor. This capacitor is the energy storage, which supplies the three-phase inverter circuit. This capacitor is also in charge of filter the input DC-Voltage.

Power flow of the whole system can be in both direction. The power can flow from the DC-Link to the motor (motoring operation) and from the motor to the DC-Link (regenerating operation). In this thesis, the power flow from the motor is not allowed. Because for a safe operation with the inverter in regeneration mode, the power must be dissipated with a brake resistor, which is absence in the used inverter. In case of power flowing in to the DC-Link the whole power will taken by transistors. Therefore, the transistors can be destroyed. This implies an acceleration of the motor speed is possible, however a deceleration is not possible in practice.

The output currents of the inverter are adjusted by pulse with modulation control, which is an efficient modulation technique. In this method a fixed dc input voltage is given to the inverter and a controlled ac output is achieved by adjusting the transistor gates. The main advantage of this method is that, low order harmonics can be minimized. With the PWM technique the phase of the currents is shifted by 120 degrees (Figure 2.4).

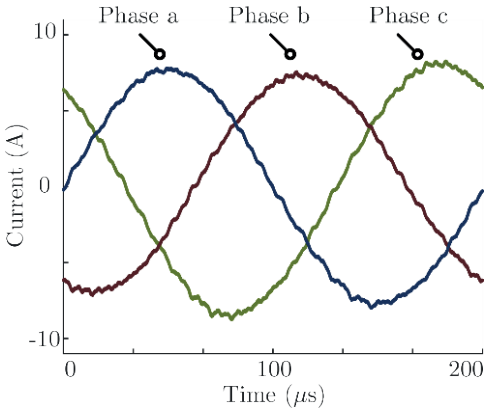

Figure 2.4: 120 degrees phase shifted currents at output of VSI

2.3 Field Oriented Control of PMSM

Sensorless motor control is based on the field-oriented control of the PMSM. Therefore, the same procedure must be made for a speed and current controller design of a motor control with a position sensor to replace the physical sensor with an observer. This controller method regulates the spatial position of the magnetic flux of the machine. This method also allows the control of the flux and torque of the machine independently of each other. The design of controller is taken from the Power Electronics System Lecture at ETH-Zurich [2]. The calculated parameter gain values are taken from a previous work, which are calculated already. However, the controller design procedure is recapitulated in case for the observer design.

2.3.1 Principle

A known standard ac motor control in industry applications is the field oriented control for speed and torque control. This motor control has the ability to separate the control of the flux and the torque. The controller structure is a cascaded controller, which two different controllers is connected in serial. The outer controller is the speed controller, which takes as input the speed reference and regulates the synchronization current accordingly. The inner controller is the current controller, which regulates the terminal voltages at the stator.

In field-oriented controller, the measured phase current is translated into dq- frame. The benefit of this transformation is the dq frame rotates with the rotor position angle, so that the phase current acts like DC currents, which is not dependent on the rotor position. Through dq-transformations control of the currents is made easier. As explained before, the d-component of the current is proportional to the flux and the q component is proportional to the torque as shown on equation 2.9. With this approach the magnet flux and the torque of the rotor is separated.

The diagram of the field-oriented controller is illustrated in figure 2.5. The measured phase currents are transformed into dq coordinates through the angular of the position sensor with the Park equations (Eq. 2.6). A PI-Controller is used for both controller. The proportional (P) part of the PI-Controller reduces the offset value of the error quantity and responses slowly. The integral (I) part of the PI-Controller responses fast to reduce the error input of the controller, however it causes overshooting. With this consideration an appropriate design rule for the gain parameter of the controller must be determined. These parameters are defined in the forthcoming section. The outputs of the current controller are then transformed back in *abc* frame and fed to Pulse Width Modulation (PWM). Finally, PWM switches the transistor on the VSI to produce three phase sinusoidal voltages on the motor terminal.

2.3.2 Current Controller Design

To generate a sinusoidal current at the inverter output, a current controller design is required. In this part of the report, the plant of the controller is shown and required control parameter is determined. The block diagrams of the current controller loop are shown in the Figure 2.6. Both the q and d current controller will be considered as the same, so both controller will have the same controller parameters, due to simplicity.

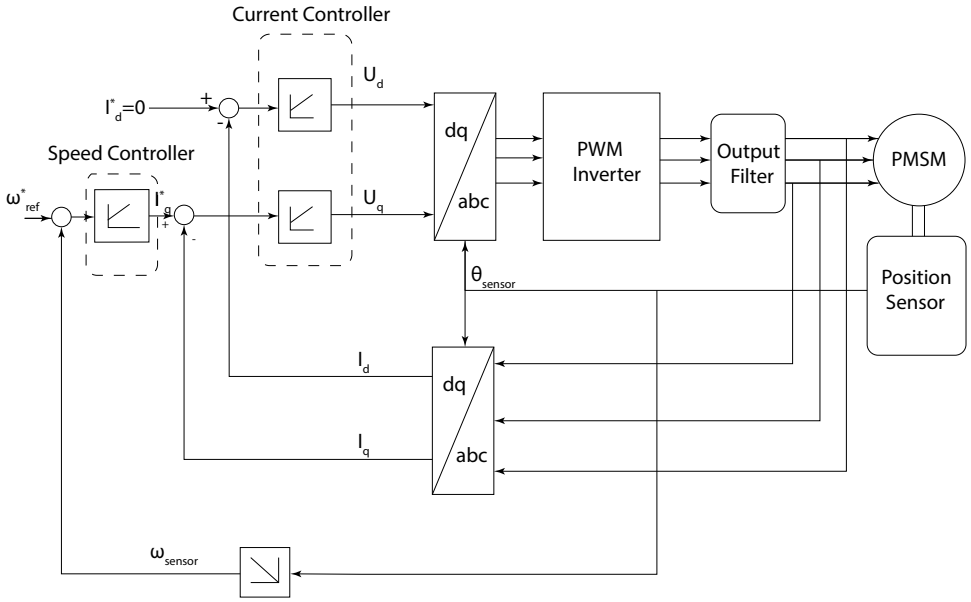

Figure 2.5: Block diagram of the applied field oriented controller

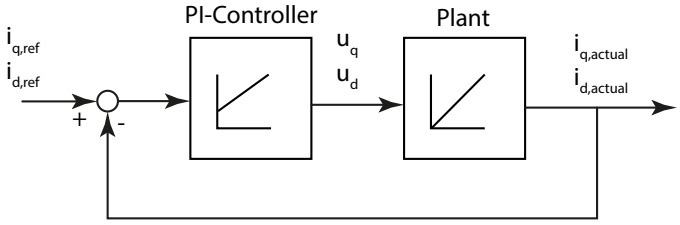

Figure 2.6: Decoupled plant for current controller

Two reasonable design rules for the current controller are given below:

1. The crossover frequency ($f_{crossover}$) of the open loop transfer function must be ten times smaller than switching frequency ($f_s = 270kHz$).
2. Phase margin must be 77° to enhance the phase margin stability criteria.

For both current controller the plant is shown in equation 2.11:

$$G_i(s) = \frac{i_d}{u_d} = \frac{i_q}{u_q} = \frac{1}{sL}, \tag{2.11}$$

A PI controller is shown in equation 2.12:

$$G_{PI}(s) = k_{p,current} + \frac{k_{i,current}}{s} \tag{2.12}$$

where the $k_{p,current}$ is the proportional gain and $k_{i,current}$ is the integral gain of the PI-Controller. With the equations 2.11 and 2.12 the open loop and the closed loop transfer function is calculated below and the bode plots and step response of the open loop function is shown in figure 2.7 :

$$G_{i,o}(s) = G_{PI}(s)G_i(s) = (k_{p,current} + \frac{k_{i,current}}{s})\frac{1}{sL} \tag{2.13}$$

$$G_{i,c}(s) = \frac{G_{PI}(s)G_i(s)}{1 + G_{PI}(s)G_i(s)} = \frac{1 + s\frac{k_{i,current}}{k_{p,current}}}{1 + s\frac{k_{i,current}}{k_{p,current}} + s^2\frac{L}{k_{p,current}}} \tag{2.14}$$

With the design criteria of above we can calculate the current controller parameters according to equations 2.15 and 2.16 ,which are shown in the table 2.1.

$$|G_{i,o}(j2\pi f_c)| = 1 \ , \ f_c = \frac{f_s}{10} \tag{2.15}$$

$$arg(G_{i,o}(2\pi f_c)) = -PM \ , \ PM = 77^\circ \tag{2.16}$$

Parameter	Value
$k_{i,current}$	160
$k_{p,current}$	0.1

Table 2.1: Current controller gain parameter

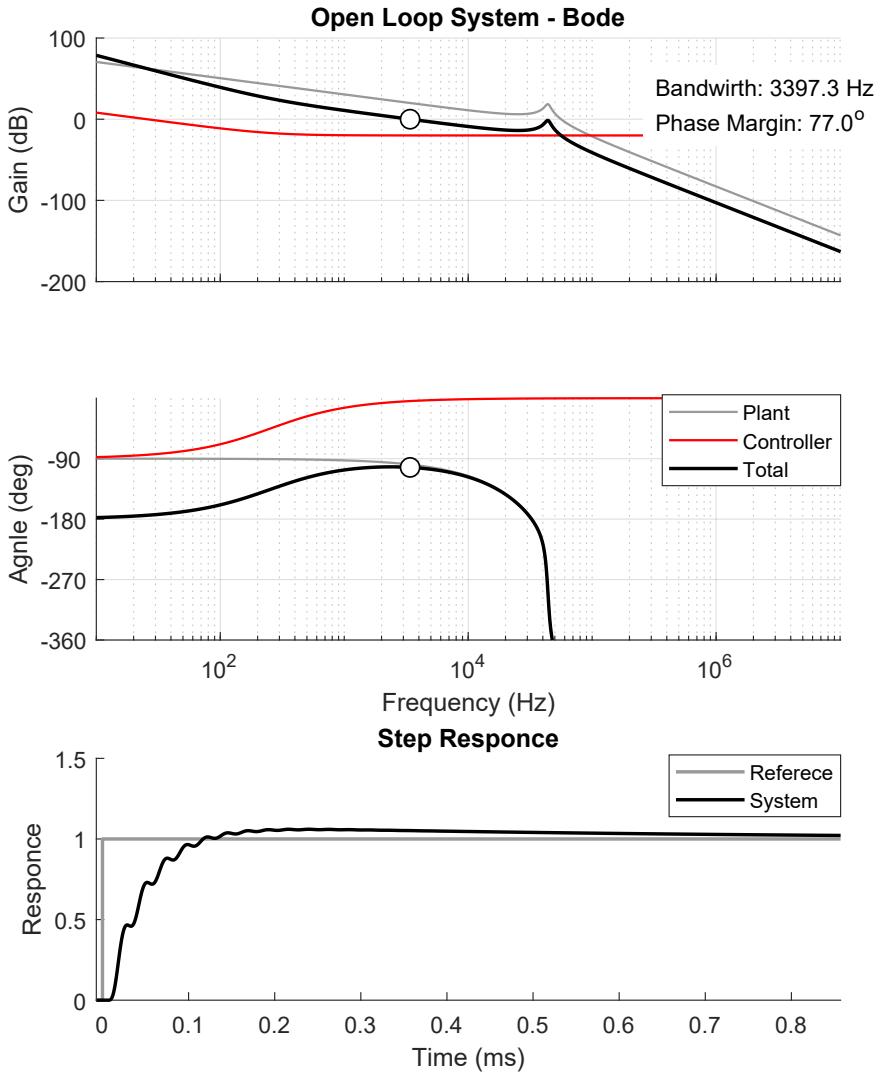

Figure 2.7: Open loop transfer function of the current controller and the step response

2.3.3 Speed Controller Design

In cascaded motor control the q component current controller is extended with speed controller. To get the appropriate q component of the current, the difference of the reference speed and actual speed is fed to PI-Controller.

To calculate the plant of the speed controller the closed loop current controller is simplified to a low pass filter. This will simplify the speed controller design procedure. For high frequencies, the closed loop transfer function shows $-20dB/dec$ decreases. So, cut-off frequency (f_c) of the low pass filter can be determined by using interpolation the bode plot. Therefore, the gain of the closed loop transfer function at the frequency of 10 times switching frequency (f_s) is calculated and using the

interpolation method the crossover frequency is obtained.

$$|G_{i,c}(j2\pi(10f_s))| = -20log(\frac{(10f_s)}{f_c}) \tag{2.17}$$

With the equation 2.17 f_c is can be calculated as:

$$f_c = 10^{(log(2\pi(10f_s))-\frac{|G_{i,c}(j2\pi(10f_s))|}{20})} = -20log(\frac{(10f_s)}{f_c}) \tag{2.18}$$

The simplified transfer function is then shown below:

$$G_{i,c} \approx G_{i,simp(s)} = \frac{1}{1+\frac{s}{2\pi f_c}} \tag{2.19}$$

With the mechanical equations of the PMSM, the electrical torque and the simplified current controller the plant of the speed (G_{speed}) is obtained:

$$G_{speed} = G_{i,simp(s)}(\frac{3}{2}\psi_p\frac{1}{sJ}) \tag{2.20}$$

where the J is the motor inertia.

The PI-Controller for the Speed Controller is shown below:

$$G_{PI}(s) = k_{p,speed} + \frac{k_{i,speed}}{s} \tag{2.21}$$

With the equations 2.20 and 2.21, the open loop transfer function of the speed controller is written as

$$G_{speed,o}(s) = G_{PI}(s)G_{speed} = (k_{p,speed} + \frac{k_{i,speed}}{s})(\frac{1}{1+\frac{s}{2*pi*f_c}})(\frac{3}{2}\psi_p\frac{1}{sJ}) \tag{2.22}$$

With the symmetric optimum criteria [3], the controller coefficients can be determined. In this method, the crossover frequency of the simplified current controller is placed at a position, where the phase gain is maximum. This method shows high overshooting at low frequency; however, the error of the speed is regulated fast.

At the crossover frequency the magnitude of the open loop function decreases with -20 dB/dec and after cut-off frequency of the low pass filter the decay is then -40 dB/dec. The cross over frequency ($f_{cross,speed}$) is place in the middle between the cut-off frequencies of PI-Controller and simplified speed controller at logarithmic scale. And the relation of these frequencies is shown below:

$$f_{cross,speed} = \frac{1}{\alpha}f_c \text{ and } f_{PI} = \frac{1}{\alpha^2}f_c \tag{2.23}$$

where f_{PI} is the cut-off frequency of the PI controller and α is a adjusting parameter to place the crossover frequency $f_{cross,speed}$.

With given design criteria following equations can be solved and the speed controller gain parameters can be calculated:

$$|G_{speed,o}(j2\pi f_{cross,speed})| = 1 \tag{2.24}$$

$$arg(G_{speed,o}(2\pi f_{cross,speed}) = -PM \ , \ PM = 70.7^{\circ} \tag{2.25}$$

With the equation 2.23 and 2.25 the α can be calculated as:

$$\alpha^2 - 2tan(\pi - PM)\alpha - 1 = 0 \tag{2.26}$$

With a phase margin of 70.7 degree α is found 0.1763 and the speed controller gain parameters are calculated and shown in Table 2.2. The bode plots and step response are shown on 2.8.

Parameter	Value
$k_{i,speed}$	0.0025
$k_{p,speed}$	0.0015

Table 2.2: Speed controller gain parameter

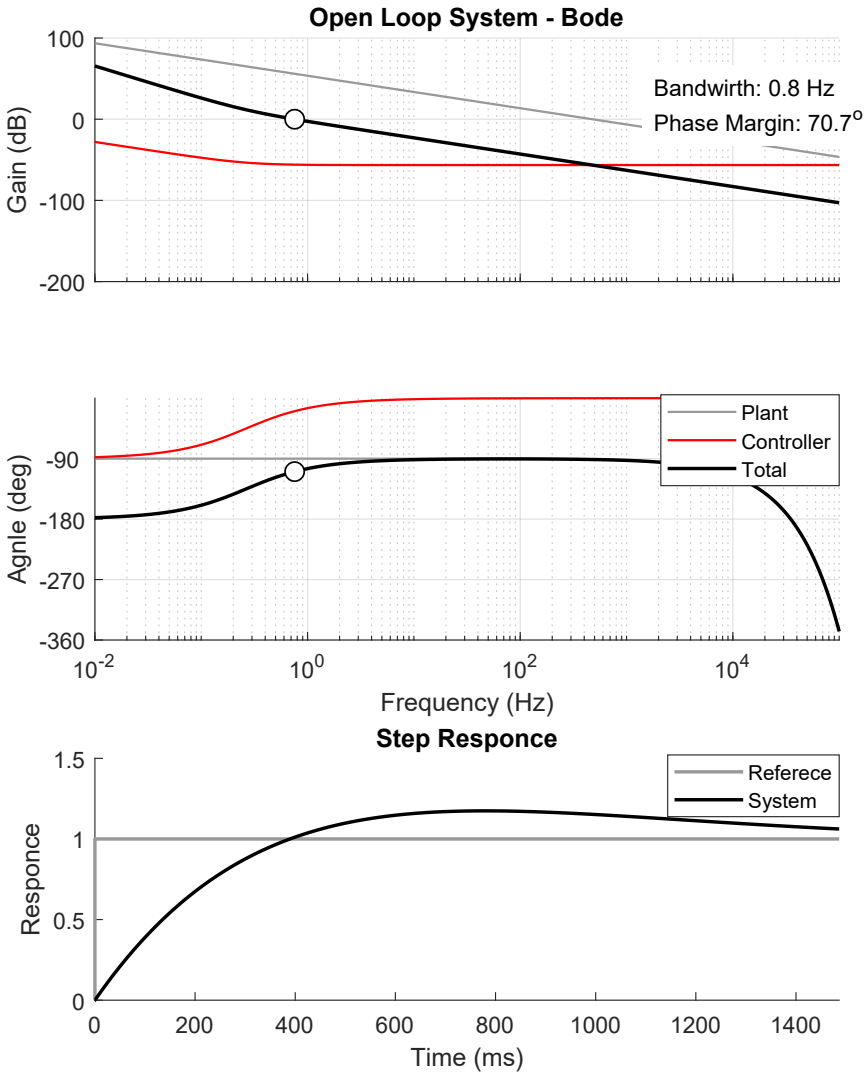

Figure 2.8: Open loop transfer function of the speed controller and the step response

2.3.4 Discrete Time Implementation and Antiwindup for FOC

The design of the controller is obtained in continuous time domain. However, the implementation of the controller is made on a DSP, which the controller must be discretized. Therefore, a discrete time implementation is needed. To enhance the integral part of the controller a backward Euler formula is used. The equation of the backward Euler respective to the PI-Controller of the previous section is shown below:

$$x_{I_{out}}[k] = x_{I_{out}}[k-1] + T_{sample} x_{I_{out}}[k-1] \tag{2.27}$$

$$y_{PI_{out}}[k] = k_I x_{I_{out}}[k] + k_P x_{p_{out}}[k] \tag{2.28}$$

To prevent any high currents or voltages at the terminal of the machine or on the electronic part, an antiwindup (Fig.2.9) is needed. Antiwindup adds limit on the controller, so the controller outputs cannot exceed these limits. The limits for speed and current controller is shown on table 2.3.

Limits	Value
Speed high limit	50000
Speed low limit	-50000
Current high limit	12
Current low limit	-12
Voltage high limit	24
Voltage low limit	-24

Table 2.3: Limitations for the speed and current controllers

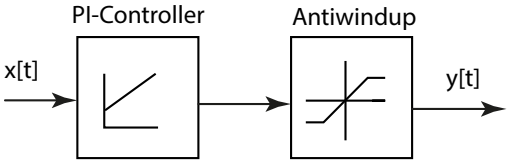

Figure 2.9: Antiwindup

Chapter 3

Sensorless Motor Control

This chapter deals with position and speed estimator methods, which can replace the position sensor device of the BacktoBack (B2B) Motor of Celeroton AG. At the beginning of this chapter an introduction to the position and speed observer is provided. Different methods are found in the literature and applicable methods are examined. From different type of observers, the most appropriate observer type is chosen, namely Phase Locked Loop Observer(PLL). PLL-Observer is in detail examined and designed for a nominal speed up to 350 $krpm$ to fulfill the requirement of the B2B Motor.

3.1 Position Observer

Most of position sensors can sense the position of the motor up to a certain speed. The realization of position sensor is complex and expensive. The motor itself is highly dependent on position sensor, so the motor reliability and robustness are reduced by the position sensor. All these drawbacks can be eliminated with "Sensorless Motor Control", which is an algorithm that estimates the position and speed of the Motor. The position estimation is based on phase currents and voltages besides motor parameter. In literature, position estimator for motors is referred as "Observer". The observer algorithm is just implemented on a DSP and the position sensor is replaced.

In literature, different type of observer is researched. Each observer type has its own pros and cons. The challenge of choosing the right observer type for this project is that, an observer type for ultra-high-speed range are very few in literature. Therefore, criteria for ultra-high-speed motors are determined for this project and different observer types are examined according to these criteria:

1. Criteria - Good Performance at high speed range: The motor, which is used in this project has a nominal speed of 350 $krpm$. Therefore, the observer must give the right position and speed at high speed range.

2. Criteria - Less computational time on DSP: If an observer is used, which is depended on the phase measurement, then the resolution must be high enough for current and speed controller. This is done with high interrupt frequency on a DSP. However, increasing the interrupt frequency will reduce the CPU execution time and the observer might not have enough time for execution. Therefore, the chosen observer must have less computational time on the DSP.

3. No physical changes on hardware: This will cause additional cost for the project. Fortunately, the phase measurements of VSI are presented in this project, in case of using an observer, which uses the phase measurements.

4. No parameter changes on current and speed controller: This criterion is not necessary, but desired. Otherwise, the current and speed controller must be considered.

In this thesis, the most important observer types are listed according to design criteria, which is an alternative to each other and at the same time a combination with each other is possible. Therefore, any other observer types are not mentioned in this thesis.

Phase Locked Loop Observer: This observer type is just based on d-component of the voltage equation of the PMSM [4]. It calculates an error quantity, which includes the position error. With a PI- Controller, the speed and position can be estimated. Due to low computational time on CPU and good performance at high speed range, this observer type is chosen for implementation on DSP. The drawback of this observer is at low speed range, because it has a exceed speed at low speed range, due to its controller gain parameter. A detail description of this observer will be discussed in a separate section.

Model Reference Adaptive Systems (MRAS): This observer type is a model based observer, which the PMSM equations, phase voltages and currents are used for the model [5]. MRAS-Observer consist two different model. One model is named as reference model, which is in *abc*-Coordinate. The second model is named as adjustable model, which is in dq Coordinate. The reference model is also referred as voltage model, because this model uses voltage equations of the machine. The reference model is referred as current model, because this model uses current equation of the machine [6]. The main idea of this observer type is, two model output are compared and an adaptation mechanism is built to extract the position error. From the output mechanism the speed and position of the motor is estimated with PI-Controller. The gain parameters can be constant or adapted with the estimated speed. The reference model can be corrected after the comparison with adjustable model with a PI-Controller. The advantage of this observer is that, it is simple to implement on a DSP and the corrected reference model, which is not the case at the PLL-Observer[7]. This observer type is an alternative for PLL-Observer and can be used as a combination with PLL-Observer and Signal Injection Method.

Kalman Filter: Kalman Filter Observer is a state observer, which is built with a nonlinear system to estimate the new states. The nonlinear system is linearized for the Kalman filter observer. The estimation is first predicted on previous states and then a gain matrix is calculated to correct the estimated state. This observer type shows high accuracy and robustness . An important feature of this type of observer is, it takes all state and allows to estimate the position and speed at low speed range, however it is complicated and needs heavy computational time. Therefore, this observer type is unfavored, due to heavy CPU usage. Extended Kalman Filter is just the nonlinear approach of the Kalman Filter. This observer type is an alternative for PLL, if the DSP has enough computational time[8].

Signal Injection Method: This observer type uses the feature of geometrical asymmetric of rotor. At an asymmetric motor the inductance in d and q direction is different. A frequency test signal is injected into stator voltage and the informa-

tion of the rotor position is extracted from current response. This method can be combined with the PLL-Observer to improve the performance[4].

3.2 Phase Locked Loop Observer

After analyzing different type of position and speed observers, the Phase Locked Loop Observer is chosen to implement on the DSP. In this part of thesis, the PLL Observer is handled in detail and requirements for the PLL-Observer are defined. The PLL Observer is shows a stable behavior in steady state.

3.2.1 General Structure of the PLL-Observer

Phase looked loop is a non linear algorithm, which detects the phase difference between signals. This algorithm is known on different areas. However, this concept is also used in motor control for speed calculation, which is based either on sensor measured position or observer estimated position.

In sensorless motor control, PLL-Observer calculates a error signal, which includes the position error of the motor. The position error is referred to the difference value between actual rotor position and observer position. Once the error signal is calculated, the position error can be extracted to estimate the speed and position.

The error signal of the PLL algorithm in sensorless motor control ε is a function of the estimation error of the observer ($\Delta\theta = \theta - \widehat{\theta}$). This function can be written in this form:

$$\varepsilon = K sin(\Delta\theta) \tag{3.1}$$

where K is a parameter, which helps to extract the position error and is referred as application specific gain parameter [9].

If the $\Delta\theta$ is assumed very small, then the error signal can be considered as linear proportional to the position estimation error:

$$\varepsilon \approx K\Delta\theta \tag{3.2}$$

Once the error signal is determined, the estimated position can be determined with physical law relation between the speed and position:

$$\frac{d\widehat{\theta}}{dt} = \widehat{\omega}_r + k_1\varepsilon \tag{3.3}$$

$$\frac{d\widehat{\omega}_r}{dt} = k_2\varepsilon \tag{3.4}$$

where $\widehat{\omega}_r$ is the estimated speed of the rotor, $\widehat{\theta}$ is the estimated position of the rotor, k_1 and k_2 are the gain parameters[9].

The entire structure above can be abstracted to PI-controller, k_1 and k_2 can be considered as k_p and k_i, where k_i and k_p are gain parameters of the PI- controller.

$$k_1 = k_i \ , \ k_2 = k_p \tag{3.5}$$

A typical PLL-Observer for sensorless motor control is illustrated in Figures 3.1 and 3.2:

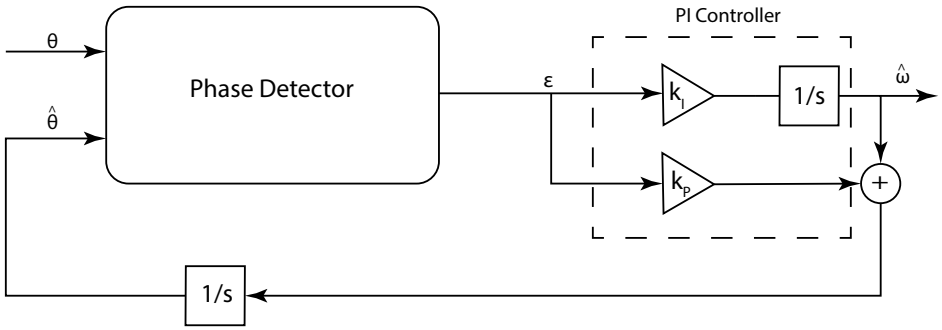

Figure 3.1: PLL structure type 1 (estimated speed is output of the integral part of the PI controller)

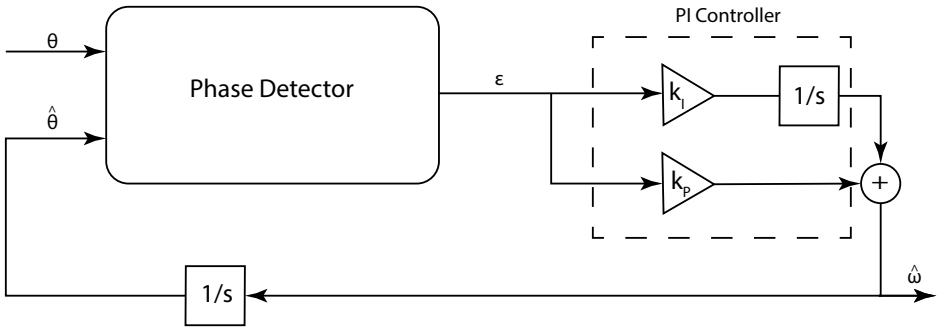

Figure 3.2: PLL structure type 2 (estimated speed is output of the entire PI controller)

Phase detector block calculates the error signal according to the estimation method. The error signal is fed to the PI-controller to estimate speed. Speed can be calculated in two ways. The speed can be calculated either as the output of the integral part of PI controller or as the output of the entire PI controller. In this thesis, the PLL-Observer is divided into two types regarding to speed calculation and both types are used.

To determine the dynamics of both PLL-Observer the transfer function of the both PLL-Observer will be calculated. Using the equations 3.2, 3.3 and 3.4 the transfer function of both PLL-Observer can be written as:

$$\frac{\widehat{\omega}_r(s)}{\omega_r(s)} = \frac{k_1 K}{s^2 + k_2 K s + k_1 K} (1.\text{Type PLL}) \tag{3.6}$$

$$\frac{\widehat{\omega}_r(s)}{\omega_r(s)} = \frac{k_2 K + k_1 K}{s^2 + k_2 K s + k_1 K} (2.\text{Type PLL}) \tag{3.7}$$

Both transfer functions show the same characteristic polynomial, which is shown below:

$$s^2 + 2s\rho + \rho^2 \tag{3.8}$$

From the equation 3.8 the gain parameters can be calculated as:

$$k_1 = \frac{\rho^2}{K} \tag{3.9}$$

$$k_2 = \frac{2\rho}{K} \tag{3.10}$$

The application gain parameter K and the bandwidth of the PLL-Observer ρ will be calculated in next section according to estimator method.

According to the transfer functions of the 1.Type PLL-Observer, the dynamic of the 1.Type PLL-Observer is slower than the 2.Type PLL-Observer. However, the 2.Type PLL-Observer has higher overshooting then the 1.Type PLL-Observer. This is a typical behavior of PI-Controller regarding the I- and PI-Output of the controller.

3.2.2 Back-emf estimator (Phase Detector Block) and Controller Design

In this chapter an estimator method will be explained based on Back-emf feature of the PMSM and the controller design is made in this section.

Back-emf (electromotive force) is a voltage that occurs in the opposite direction to the applied voltage on stator of machine. This occurs if a rotating armature is present in a presence of a magnetic flux. The position of the motor will be estimated on the back-emf equation.

To determine the error signal the d-Component of the voltage equation is applied. The voltage equation of PMSM dq-Coordinate is rewritten below:

$$u_d = i_d(R_s + sL) - \omega_{el} L i_q + \omega_{el}\psi_q \tag{3.11}$$

To regulate the position estimation error to zero, an equivalent controller structure has to be determined. This is done by abstracting the PLL-Observer in another form. This abstraction is reached in following steps:

1. Regulating the estimated position of the rotor to the actual position is equivalent to regulate the q component of the magnet flux to zero and d component of the magnet flux to its amplitude (Figure 3.3).

$$\theta \longrightarrow \widehat{\theta} \equiv \psi_q \longrightarrow 0 \text{ and } \psi_d \longrightarrow |\psi| \tag{3.12}$$

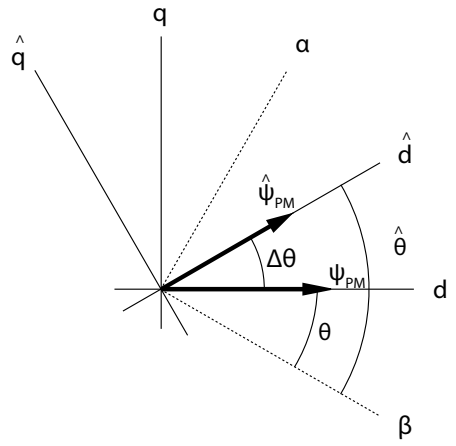

Figure 3.3: Illustration of the estimated position error

2. q-component of the magnet flux can be regulated to zero with a reference input, which is also zero. An appropriate equation for a control design can be written below with the multiplication of the speed:

$$[\omega_{el}\widehat{\psi}_{q,ref}=0]-[\omega_{el}\widehat{\psi}_q]=-\omega_{el}\widehat{\psi}_q=-\omega_{el}\widehat{\psi}sin(\widehat{\theta}-\theta)=\omega_{el}\widehat{\psi}sin(\theta-\widehat{\theta})\approx\omega_{el}\widehat{\psi}(\theta-\widehat{\theta}) \tag{3.13}$$

With the equation 3.13 the K parameter is found:

$$K=\omega_{el}\widehat{\psi} \tag{3.14}$$

The control diagram of equation 3.13 is shown below

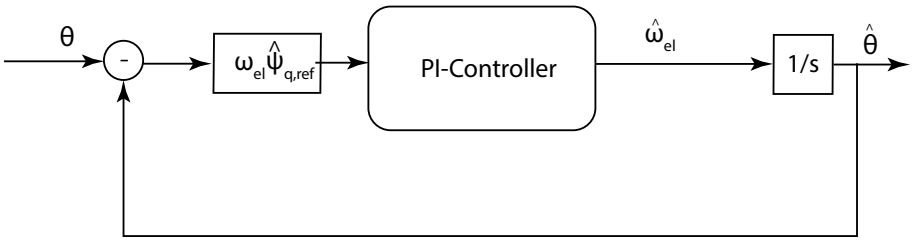

Figure 3.4: Abstracted equivalent control structure for PLL-Observer

3. If the d-component of the voltage equation of the PMSM (Eq. 3.11) is taken and recalculated, a magnet flux dependent equation 3.15 is found to abstract the position estimation. This equation (Eq. 3.11) is the same equation 3.13 and a way is found for calculation the error signal in the Phase Detector Block 3.5.

$$-\omega_{el}\widehat{\psi}_q=i_dR_s+sL-\omega_{el}Li_q-u_d \tag{3.15}$$

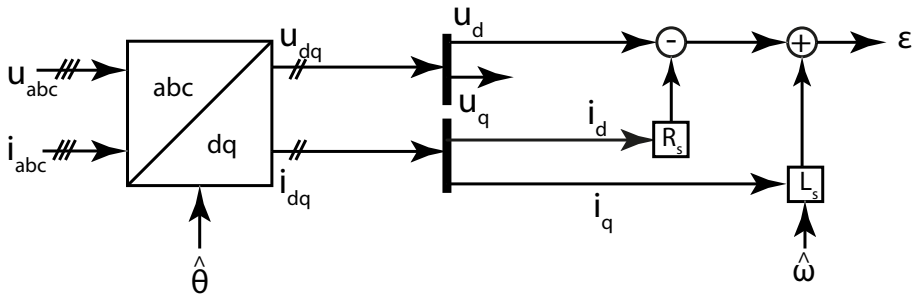

Figure 3.5: Phase detector unit

Finally, with the back-emf estimator the error signal quantity is calculated, by using the phase current and voltage measurements. This is an intended feature, because it does not require any changes on the hardware of the VSI. Another advantage of the PLL-Observer is that, it is based on one equation, so that the calculation of the position and speed estimation is simple. This enhance low CPU usage feature on DSP, which lots of observer types do not have. Although to calculate the estimated position and speed is not enough, it needs also a controller design to have stable behavior to replace the physical sensor device.

To complete the PLL-Observer a gain parameters of the PI-Controller must be found. The PI controller can be written in their classical form. However, the PI controller will be used with a low pass filter [10]. The PI controller with a filter can be written in this form:

$$G_{PIcontr.} = (\frac{1}{sT_f})(kp + \frac{ki}{s}) \tag{3.16}$$

With PI controller the closed loop transfer function of the PLL observer can be written as:

$$G_{cl} = \frac{\frac{kp}{ki}s + 1}{\frac{Tf}{ki\omega_{el}\widehat{\psi}}s^3 + \frac{1}{ki\omega_{el}\widehat{\psi}}s^2 + \frac{kp}{ki}s + 1} \tag{3.17}$$

kp, ki and Tf can be calculated according to the characteristic polynomial:

$$(sTd + 1)(s^2 + 2Dc + \rho^2) \tag{3.18}$$

, where Dc is a damping factor.
After some calculation, the transfer function from estimated speed to actual speed, control parameter gains and first order low pass filter can be written as below:

$$\frac{\widehat{\theta}}{\theta} = \frac{s(\frac{2Dc}{\rho} + \rho) + 1}{(+1)((\frac{s}{\rho}^2) + 2Dc\frac{s}{\rho} + 1)} \tag{3.19}$$

$$kp = \frac{\rho}{\omega_{el}\widehat{\psi}} \tag{3.20}$$

$$ki = \frac{\rho^2}{\omega_{el}\widehat{\psi}}\frac{1}{1 + \frac{2}{\rho}} \tag{3.21}$$

$$Tf = \frac{1}{\rho}(1 + \frac{2}{\rho}) \tag{3.22}$$

The PI controller gains are unusual not constant. The controller gains are changing with the rotor speed. This allows better control dynamics at high speed range, however for low speed range this controller gains exceeds with the decreased speed and it does not possible to run the controller in stable behavior.This will be handeld in detail in the chapter limitation and is not handeld in this chapter.

3.2.3 Discrete Time Implementation

The Phase locked loop observer, which is based on the back-emf method, has been derived in continuous time mode. However, implementing the PLL-Observer on the DSP requires sampling with the interrupt frequency. In most of observer applications the CPU usage plays an important role, because most of microcontroller has less CPU usage to run the observer code. For that reason, optimized coding must be used for observer implementation. For the implementation backward Euler method is used as the same in the chapter 2.3.4

3.2.4 Design Rules

To enhance a position estimator of PLL-Observer, the dynamics of the transfer function must be considered. For that reason, reference tracking, disturbance rejection and noise rejection analysis will made to define restriction and control parameter of the PLL-Observer.

Reference Tracking

A transient analysis and ρ selection is made in [11]. The bandwidth is given as

$$\rho = \sqrt{\frac{a_{speed}}{sin\tilde{\theta}_{max}}} \tag{3.23}$$

, where a_{speed} is the maximum of the speed acceleration and $\tilde{\theta}_{max}$ is the maximum allowed transition error of position. The maximum acceleration of the machine is assumed as 100 $krpm/s$ and the maximum allowed transition error of position is assumed about 1° for this project. Therefore, the bandwidth is calculated 794.7, but it is rounded up 800 rad/s.

Bandwidth of the Observer influences the bandwidth of the speed and current controller. The bandwidth of the observer must be sufficiently low of the current controller and sufficiently high of the bandwidth of the speed controller:

$$\rho_{speed} << \rho_{observer} << \rho_{current} \tag{3.24}$$

Disturbance Rejection

The load torque variations are another design criteria for design criteria, which determines the lower bound of the bandwidth. This is determined in [12] as:

$$\rho_{obs,min} = \frac{1}{T_{mech}} \tag{3.25}$$

, where T_{mech} ($T_{mech} = J\omega_N/T_N$) is the mechanical time constant about 0.6911 s/rad. The $\rho_{obs,min}$ is found as 1.4470 rad/s, which much lower then 800 rad/s.

3.2.5 Space Harmonics

During the PLL-observer design two kind of harmonics is considered. One harmonics is the switching harmonics. Switching harmonics is beyond the passband of the noise transfer function of the PLL-estimator. Therefore, switching harmonics has less impact [11].

A second type of harmonics is the space harmonics of the machine. Especially at low speed region the magnet and the rotor permanence generates special harmonics. The space harmonics are a result of non-sinusoidal distribution of the coils in the machine and slotting. This space harmonics determine a speed limit, where under this limit the adaptive gain parameters must be scaled down with the proportional of the speed limit. The lowest possible harmonics in synchronous machine is the 5.harmonics [11]. This must be considered on the noise transfer function from the PLL observer. The calculations are made at the simulation Chapter 4 and is not handled in detail in this chapter.

3.2.6 Limitations

For the realization of the PLL observer several limitation aspects can be concluded after previous sections.

First limitation occurs at low speed range. The PLL-Observer has a lower bond speed range to run properly. From zero speed, the PLL-Observer cannot estimate the speed and position. For that reason, the machine must be started at open loop control to a certain speed. After a certain speed is reached, the whole control structure can be changed to closed loop sensorless control.

Another limitation of the PLL-Observer occurs from the estimation method. The estimation method is model based, which includes parameters like resistance and inductance. These parameters are temperature depended and with the increased speed the motor temperature will increased and so the parameter of the model will be changed. This is an uncertainty of the PLL-Observer, which is considered in the next chapter.

Chapter 4

Simulation Setup and Results

To realize the phase locked loop observer a couple of simulation is required to verify the validation of the sensorless control system. An existing VSI-Inverter and motor model are built on the Gecko-Circuit tool. Additionally to these models, both type of PLL-Observer are built in Matlab-Simulink for this project. These two simulation tools are interconnected and the simulations are made for different operating points (Figure 4.1). At the end of this chapter, an uncertainty analysis is made to determine the robustness of the PLL-Observer.

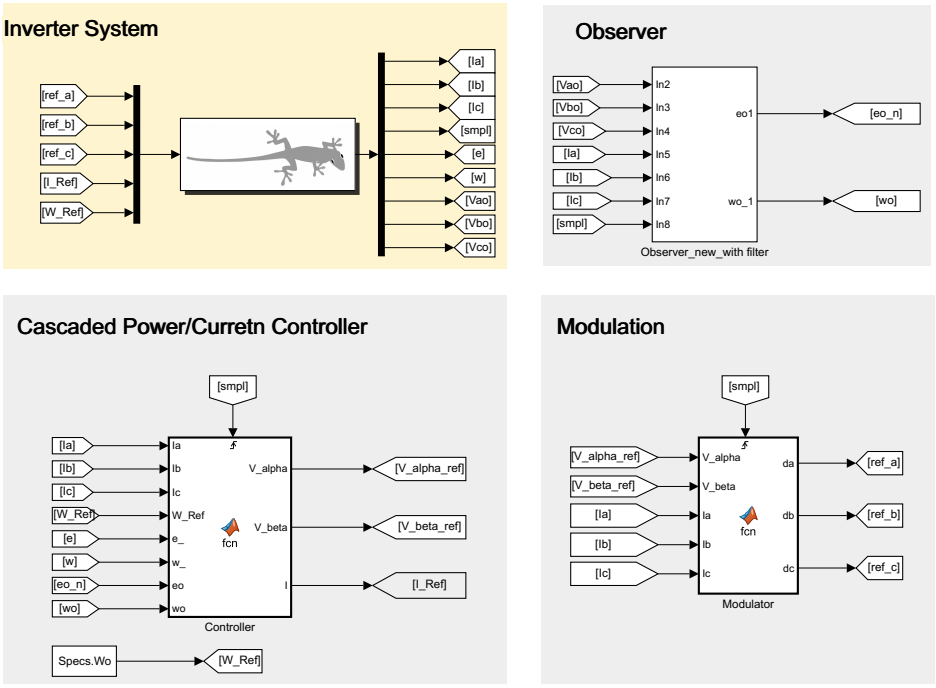

Figure 4.1: Simulink block diagram of the sensorless control system

The nominal parameters of the VSI-Inverter and PMSM are shown in Table 4.1 and 4.2. This parameters are taken from the experimental setup of this project (Chapter 5). Therefore a specific simulation models are built for this project.

Parameter	Value
Switching Frequency (kHz)	140
DC Link Voltage (V)	48
Filter Inductance (μH)	18
Filter Capacitor (μF)	0.66
Damping Capacitance Ratio	0.2

Table 4.1: Parameter of the VSI

Parameter	Value
Motor Nominal Speed ($krpm$)	350
Motor Inductance (μH)	4.72
Motor Resistance ($m\Omega$)	39
Flux Linkage (Wb-t)	0.63
Machine Rotor Inertia (kgm^2)	96e-9
Motor Rated Torque (Nm)	11

Table 4.2: Parameter of the PMSM

The controller part of the simulation system is a cascaded controller as described in the Chapter 2.3. The speed controller and current controller parameters is shown in Table 4.3. The modulation process for the transistor switches is made with PWM Sinusoidal Technique.

Parameter	Value
$k_{p,speed}$	0.0015
$k_{i,speed}$	0.0025
$k_{p,current}$	0.1
$k_{i,current}$	160

Table 4.3: Speed and Current Controller Gain Parameters

The simulations are performed for different initial motor speeds. To keep the simulations fast, the initial speed is given high enough and it is reduced until the control system loss its stability. In this way, an under limit for the initial speed of the PLL-Observer is determined. For improvement of the PLL-Observer speed estimation, a low pass filter is added to the observer speed in Simulink. With adding a digital filter, the initial speed speed of the 2.Type PLL-Observer is reduced significantly. The evaluated different working points for simulations are summarized in Table 4.4:

Observer Type	Initial Speed ($krpm$)
1.Type PLL-Observer without filter	1 and 50
1.Type PLL-Observer with filter	1 and 50
2.Type PLL-Observer without filter	8.5 and 50
2.Type PLL-Observer with filter	1 and 50

Table 4.4: Simulation working points

Only the simulation results with a low pass filter are shown in this report. The motor speed and position are not shown separately, because the position- and speed estimation errors is calculated according to the motor speed and position. Therefore, any conclusion about the comparison of the Observer speed and position values with the motor can be made with the estimation errors.

4.1 Simulation Results of 1.Type PLL-Observer

The lowest possible initial speed is found as 1 *krpm* for the 1.Type PLL Observer (Figure 4.5). Below this initial speed, the 1.Type PLL-Observer model is not working. Especially, the controller gain parameter of the PI-Controller is increased and can not regulate the position error. Therefore, wrong observer speed and position is fed to the speed controller and *dq*-Transformation. The entire system is then unstable with an initial speed under 1 *krpm*.

In Figure 4.2, the speed acceleration with different initial speeds is the same up to time 1 *sec*. This causes the same speed estimation error for both cases up to time 1 *sec* (Figure 4.3). For the case with higher initial speed, the acceleration of the observer speed is reduced before then the case with lower initial speed after 1 *sec*. Therefore, the speed error of higher initial speed case is reduced before then for lower initial speed case. In both cases the 2.Type PLL-Observer shows an offset value speed estimation error. This phenomena is expected, because only the output of the I-Controller of Observer is taken as observer speed. However, the offset value is reduced to about zero, when the observer speed is closer to reference speed. A total eliminating the offset value is not possible. Therefore, the estimated speed error varies with an offset value.

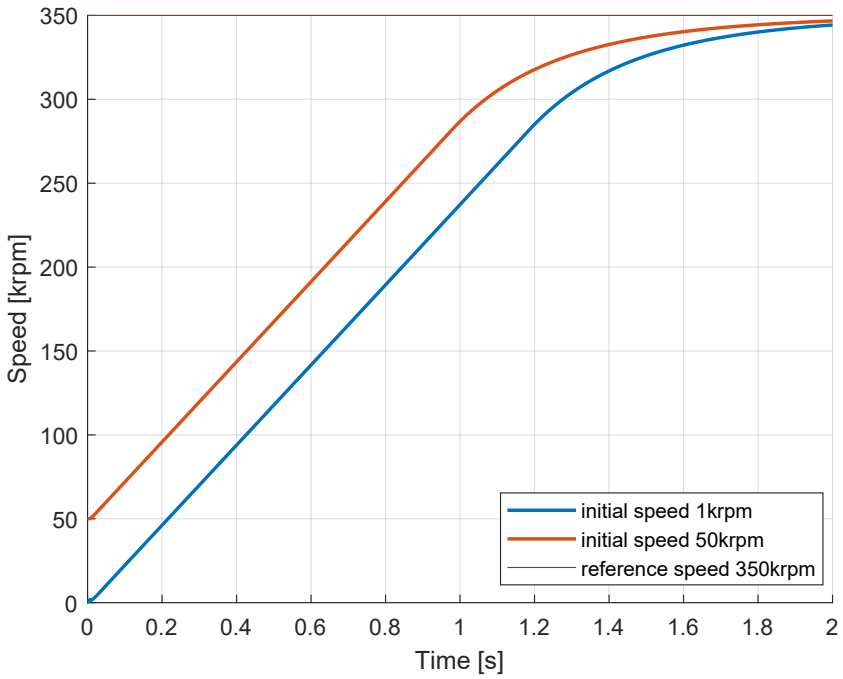

Figure 4.2: Speed estimation of 1.type PLL-Observer with filter

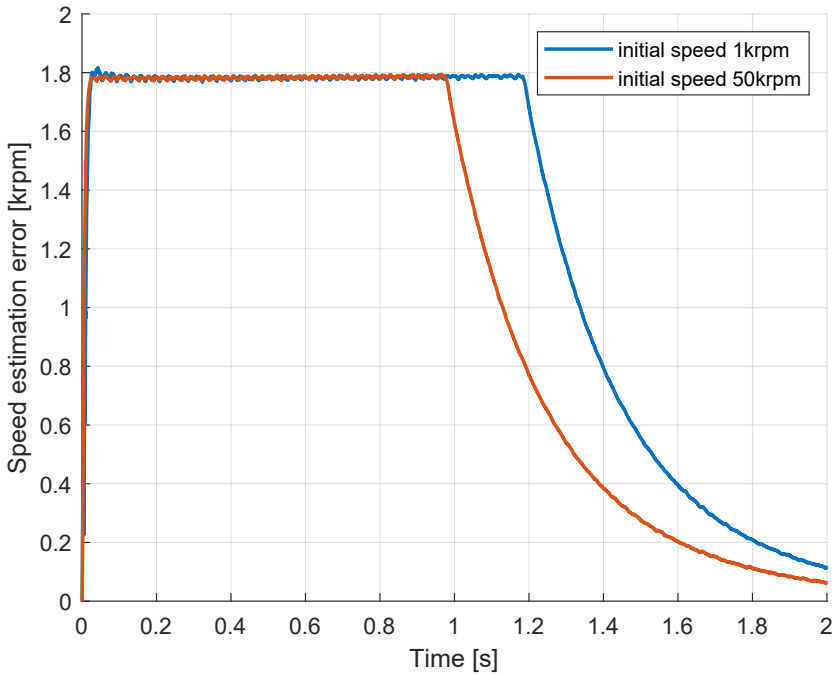

Figure 4.3: Speed estimation error of 1.Type PLL-Observer with filter

The position estimation and position estimation error of 1.Type PLL-Observer are shown in Figure 4.4 and 4.5. The offset value, which is seen for the speed error, causes for the position estimation error also an offset value. However, the position estimation error is not more than 0.1 *rad*,which is about 5 degree. At steady state, the position estimation error is very close to zero, but it remains an offset value.

An important observation is the high overshooting for the position estimation error at the beginning of the simulation in case of initial speed 1 *krpm*. Without using a low pass filter, this overshooting is higher and it is reduced with a low pass filter. The correct position is crucial for a stable system and with such high overshooting the 1.Type PLL-Observer can not be realized. Therefore, the 1.Type PLL-Observer must be realized with higher initial speed.

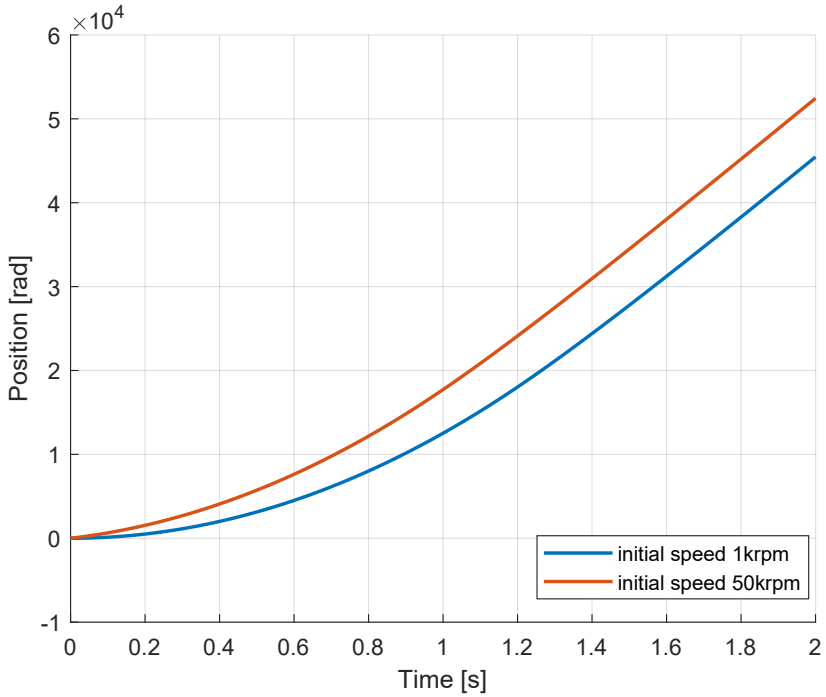

Figure 4.4: Position estimation of 1.Type PLL-Observer with filter

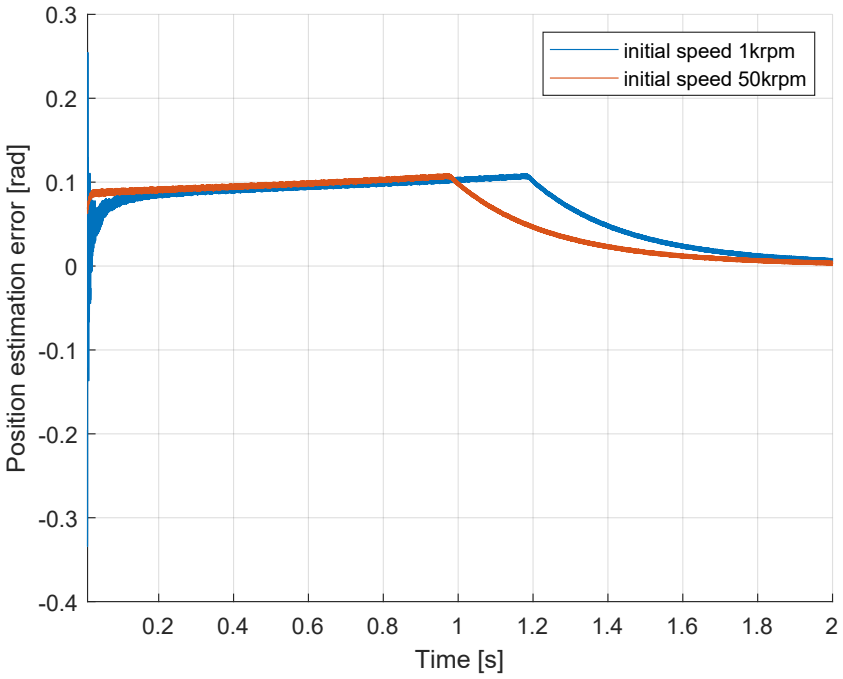

Figure 4.5: Position estimation error of 1.Type PLL-Observer with filter

4.2 Simulation Results of 2.Type PLL-Observer

Similar simulations are made for 2.Type PLL-Observer. The lowest initial speed is found as 1 *krpm* for a stable system (Figure 4.6). An observer speed below 1 *krpm* the system not stable. The speed estimation error of the 2.Type PLL-Observer is shown in Figure 4.7. The offset value of the speed estimation of the 1.Type PLL-Observer is eliminated and the speed estimation error various around zero. This phenomena is occurred, because the speed of observer is taken as output of the PI-Controller of the PLL-Observer. In case with lower initial speed, a small overshooting is occurred,while in case with higher initial speed the overshoot is very small.

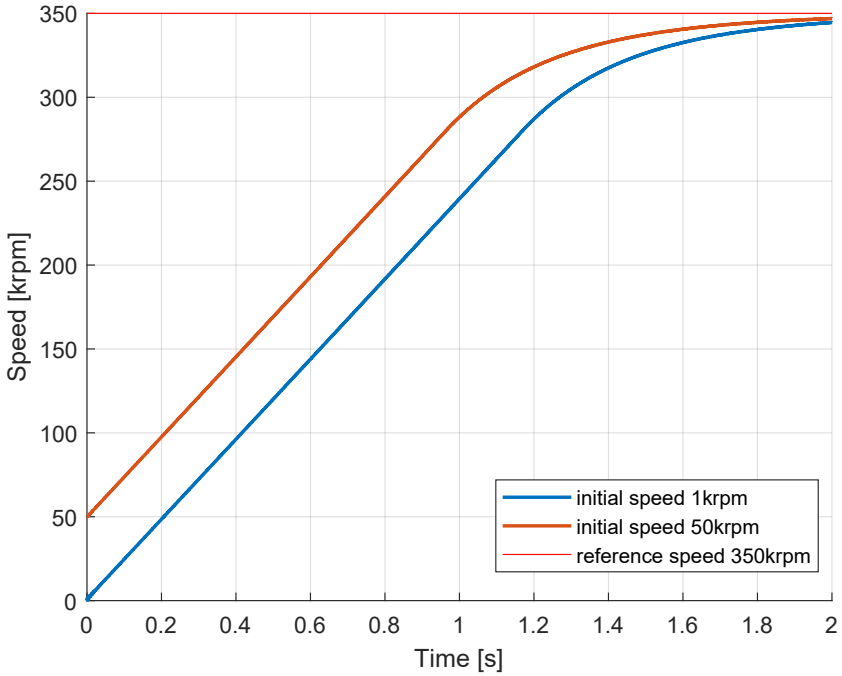

Figure 4.6: Speed estimation of 2.Type PLL-Observer with filter

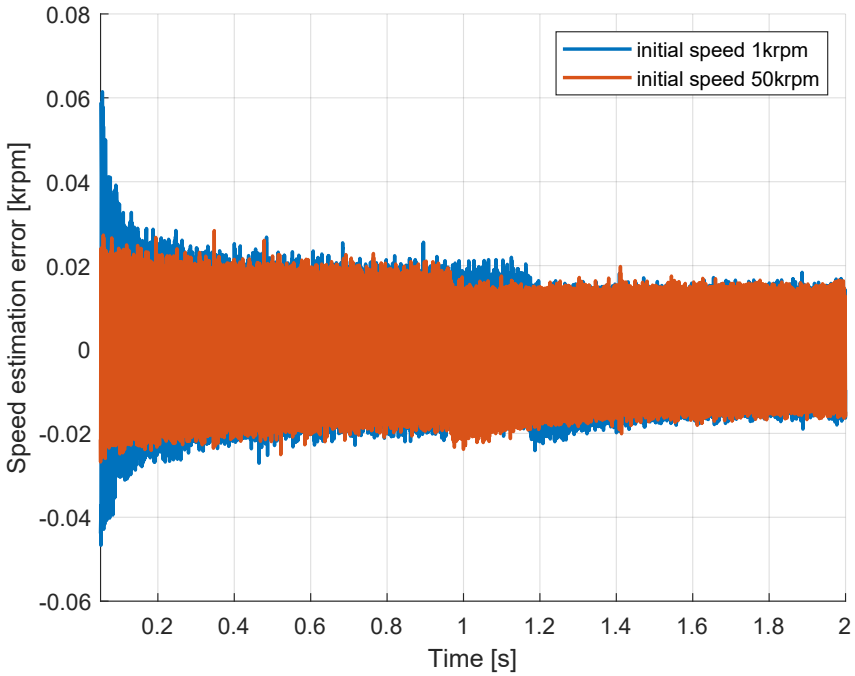

Figure 4.7: Speed estimation error of 2.Type PLL-Observer with filter

The position estimation and position estimation error of 2.Type PLL-Observer are shown in Figure 4.8 and 4.9. It is quite similar to the 1.Type PLL-Observer. The position estimation error is increased slowly for a short time, but then it is suppressed to around zero. The position estimation error is smaller than 0.02 *rad* at steady state, which is about 1,5 in degree.

The same observation is seen about the high overshooting for the position estimation error at beginning of the simulation in case of initial speed 1 *krpm*.The same statement can be made for the 2.Type PLL-Observer as 1.Type PLL-Observer and is not repeated here.

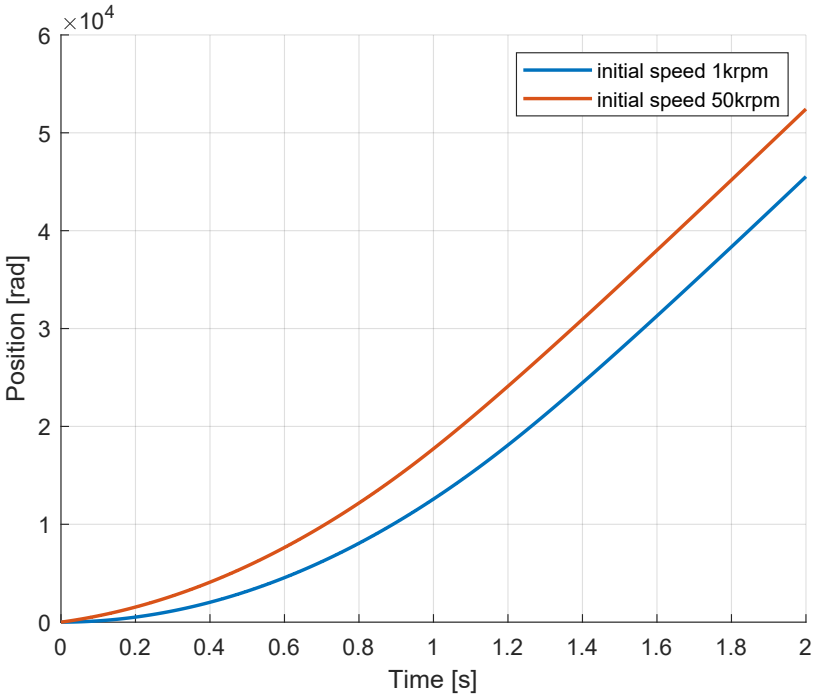

Figure 4.8: Position estimation of 2.Type PLL-Observer with filter

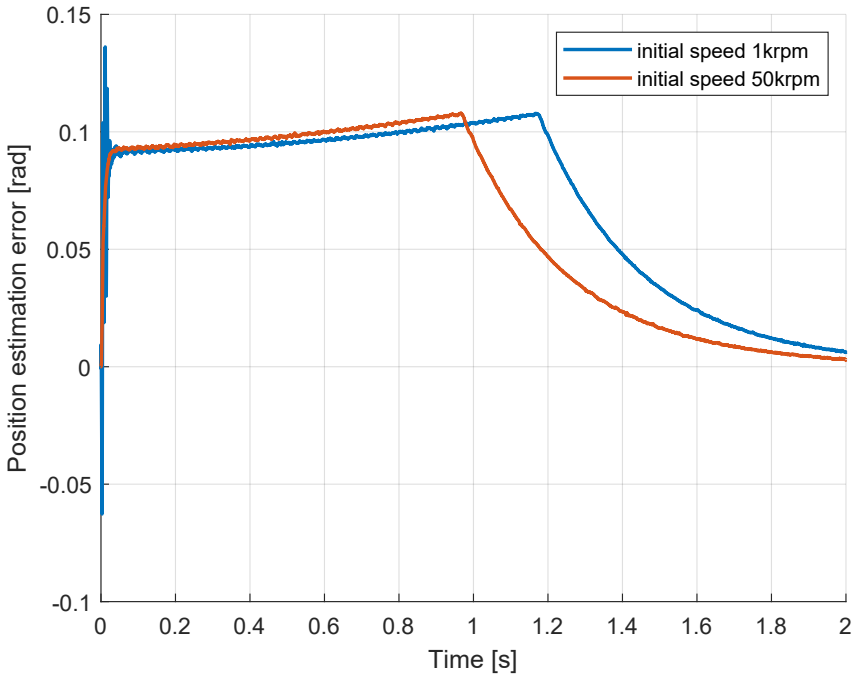

Figure 4.9: Position estimation error of 2.Type PLL-Observer with filter

4.3 Uncertainty Analysis

The uncertainty analysis of the PLL-observer determines the robustness of the observer. The uncertainty analysis is made on two bases. First base is the PLL-Observer model, which is highly dependent on the machine parameters. The second base is the measured phase current and voltages. Any changes of those parameters will change the error quantity of the PLL-Observer.

In [9], a noise analysis for the PLL-Algorithm is made and the transfer function of the noise to estimated speed error ($\tilde{\omega}$) and estimated position error ($\tilde{\theta}$) of the PLL-Algorithm is given as

$$\tilde{\omega} = -\frac{\rho^2}{K}(\frac{s}{(s+\rho)^2})n \tag{4.1}$$

$$\tilde{\theta} = -\frac{\rho}{K}(\frac{2s^2+5\rho s+2\rho^2}{(s+2\rho)(s+\rho)^2})n \tag{4.2}$$

,where the n is the noise component which added to the estimated position, where n is considered as disturbance. The transfer function 4.1 is the noise to speed transfer function and the transfer function 4.2 is the transfer function of the noise to position. The first transfer function is a band pass filter and the second is a low pass filter. The noise to speed transfer function shows a zero error at steady state, if the noise is a DC-signal. This implies that, slowly varying parameter uncertainties do not produces a speed error, however at equation 4.2 it can produce a position error in steady state[9].

With the equation 4.1,the impact of the space harmonics can be considered, which is generated by rotor permanence. The lowest possible space harmonics occur at fifth harmonic in stator coordinate and this determines a lower speed limit for the controller gain [11]:

$$\omega_\lambda > 2.5 * \rho \tag{4.3}$$

, where ω_λ is the speed limit and ρ is the observer bandwidth. Under this speed limit the bandwidth of the observer is reduced with inverse proportional to the speed limit.
For ω_{obs}>ω_λ:

$$ki = \frac{\rho^2}{\omega_{obs} * \psi} \text{ , } kp = \frac{2*\rho}{\omega_{obs}.\psi} \tag{4.4}$$

For ω_{obs}<ω_λ:

$$ki = \frac{\rho^2 * \omega_{obs}}{\omega_\lambda^2 * \psi} \text{ , } kp = \frac{2*\rho*sign(\omega_{obs})}{\omega_\lambda.\psi} \tag{4.5}$$

,where ω_{obs} is the speed of the observer. The Equation 4.5 is refereed as down-scaled controller gain parameters, if nothing else is stated. For this project the speed limit (ω_λ) is found 2000 rad/s($\approx$19000$krpm$).[1] The down-scaled controller gain parameters will be used under the speed limit for the experiments with the hardware in the next Chapter 5.

[1] In microcontroller speed limit is set to 20 $krpm$.

Another aspect is based on the motor parameters like resistance and inductance of the rotor. Any changes on these parameters can be caused by temperature or saturation. In [12], an asymptotic position estimation error is given as:

$$\epsilon_\infty = sin^{-1}(\frac{\delta L}{\psi}) \tag{4.6}$$

where δL is the parameter error on inductance. This equation 4.6 implies that, the most critical parameter is the inductance. To determine the influence of the inductance, the nominal value of the inductance is increased to its twice value. In the results has been seen, it has not much influence. Therefore, any plots of this experiment are not shown. The reason for that is the observer system is working closed loop and error dynamics is still stable with the adaptive controller method.

Another parameter is the resistance of the PMSM. This is highly depended on the machine temperature, which increases with the speed especially. However, on the error quantity the resistance is not present and is not considered further.

The uncertainty of the PLL-Observer is considered under the assumption of the correct phase voltage and current. However, it is also important to determine the influence of the noise on the current and voltage measurements. For that reason a noise signal was added to the current and voltage signal with 100 Hz and 5%. This has not showed remarkable results. It was also built a simplified model with a sinusoidal current and voltage to change the phase and voltage offset between phase current and voltages. However, a reasonable result was not found.

Another important aspect is the influence of the inverter filter. Inverter output filter is a speed reduction factor and it was researched that can be used the unfiltered voltage and current measurements to estimate the position and speed with PLL-Algorithm. Qualitatively, neither in parallel nor in serie, 1.Type PLL-Observer shows a stable behavior. However, 2.Type PLL-Observer can estimate the speed with a deviation of 0.5 *krpm* (Figure 4.10). However, the position error is getting higher, which can cause a wrong position transfer for the dq-Transformation (Figure 4.11).

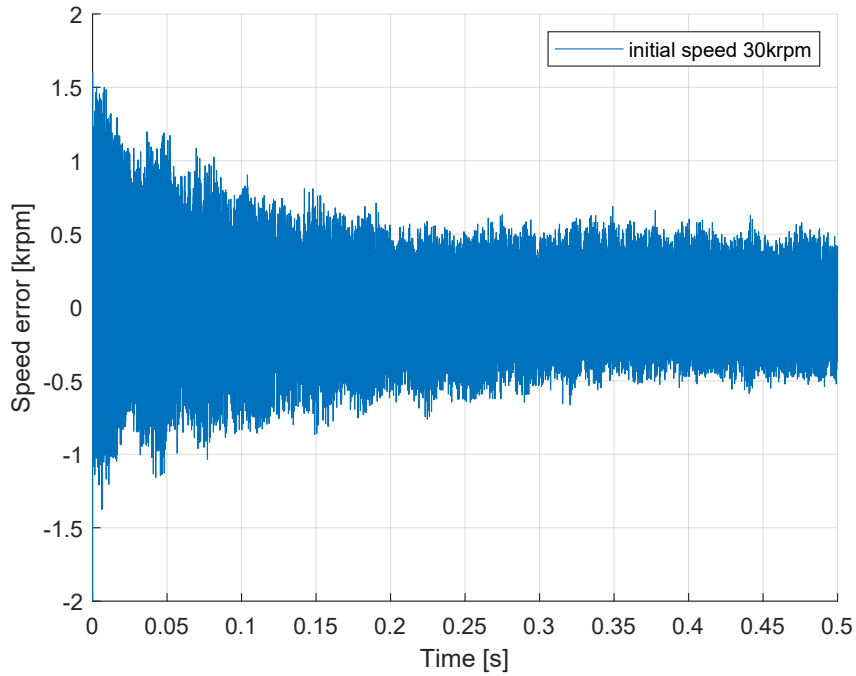

Figure 4.10: Speed estimation error of 2.Type PLL-Observer without inverter filter

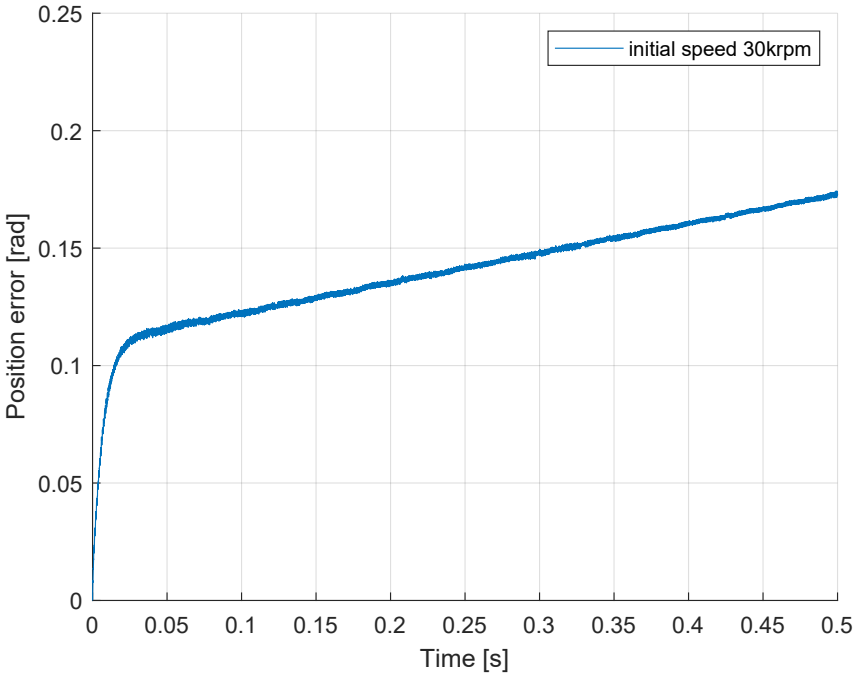

Figure 4.11: Position estimation error of 2.Type PLL-Observer without inverter filter

Chapter 5

Hardware Setup and Results

With the knowledge of the previous chapters, the PLL-Observer can be realized on a microcontroller to perform it at high speed range. In this chapter an experimental environment is built to perform the PLL-Observer. In the first part of this chapter, the setup of the experiments is introduced, which includes the electrical machine, the inverter and the controller board. The controller board will be then replaced with a controller board, which has a higher CPU-Clock frequency. In the next part of this chapter, the evaluations of the experiments are presented for different operating points.

The aim of the experiments is to run the designed PLL-Observer at nominal speed of the PMSM of Celeroton AG with the VSI-Inverter of PES-Laboratory.

5.1 Experimental Environment

The electrical machine is made by Celeroton AG (Figure 5.1). It is a PMSM and named as *Back to Back* (B2B) Motor. B2B machine has two different stator windings around the rotor. Therefore, one winding of stator can be used as a motor, while the second winding of the stator as generator and vice versa (Figure 5.2). This machine is used as a turbo compressor and parameters are shown in Table 5.1:

Parameter	B2B-1	B2B-2
Nominal Speed (krpm)	350	350
Motor Inductance (μH)	4.72	4.73
Motor Resistance ($m\Omega$)	39	39
Flux Linkage (mVs)	0.63	0.55
Rated Torque (Nm)	11	11

Table 5.1: B2B Machine Parameters

The B2B motor is equipped with a position sensor. The position sensor is constructed with four hall effect sensors, which are placed 90 degrees apart from each other around the rotor. The signals of the hall effect sensors are differentiated and transformed from analog to digital signals with an AD-Converter.

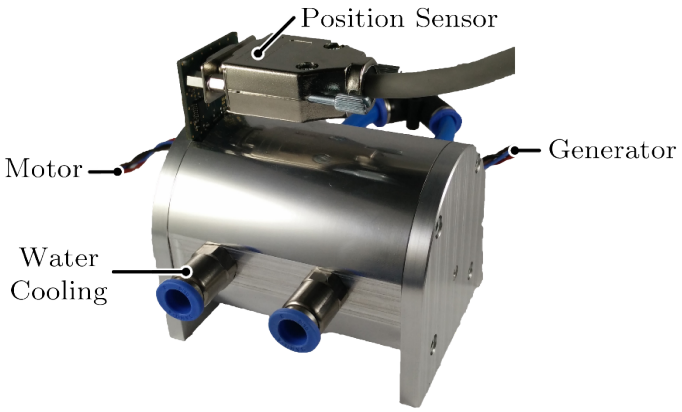

Figure 5.1: Photograph of the BacktoBack (B2B) Machine

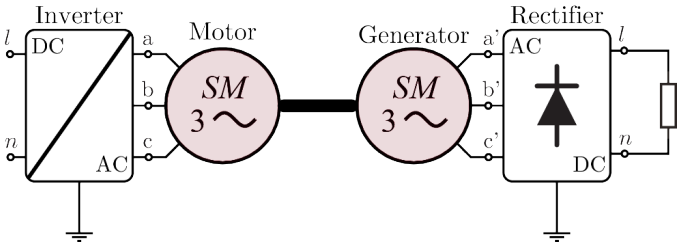

Figure 5.2: B2B working scheme

The Voltage Source Inverter (VSI) is shown in Figure 5.3. This inverter is special designed at PES-Laboratory for the B2B-Motor. It has a peak efficiency of 97%. This inverter has no brake resistor. Therefore, a bidirectional power flow is not possible. Any decreasing of the motor speed is not allowed, otherwise the power flow direction will be from the motor to the inverter and whole power will be taken from switches, which can burn them. The parameters of the VSI inverter are shown in Table 5.2.

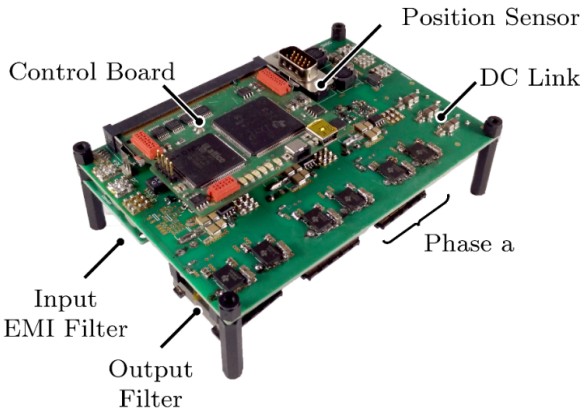

Figure 5.3: VSI Inverter

Parameter	VSI
Rated Input Voltage (V)	0-48
Rated Output Voltage (V)	0-24
Rated Output Current (A)	10

Table 5.2: VSI Parameters

The implementation of the Controller and PLL-Observer is made on Code Composer Studio, which is a development environment for TI-Micro controller, step by step:

1.Step (Controller Mode 1):

In this step, an open loop speed controller is implemented, which the frequency of the phase currents and the modulation index parameter of PWM is given as user input. In this mode, a resistor is used as a load.With this mode is ensured that, the gate signals of the microcontroller are working correctly.

2.Step (Controller Mode 2):

In this step, an open loop controller is also implemented. The q component of the current are given as user input, instead of modulation index parameter . This mode uses as output load a resistor or a machine. With this mode it is ensured that, the voltage and current measurements are working correctly. It also ensures whether the current controller is working properly.

3.Step (Controller Mode 3):

In this mode the calibration angle is calculated, which is the angle between the magnet flux of the motor and the stator windings. With this calculation an angle correction is made for the dq-Transformation. This is important, because the q component of the current and the d component of the magnet flux must be placed perpendicular to each other to generate a torque at the rotor. Without angle calibration the needed torque is not generated.

4.Step (Controller Mode 4):

This mode is the cascaded controller mode. The position sensor gives the angle, which is corrected by the calibration angle and all controller structure are working in closed loop. This mode ensures that, the speed controller is working properly. Only the speed reference is given as an user input.

5.Step (Controller Mode 5):

This mode is the same as the controller mode 3, however, instead of giving the current frequency and the q component of the controller, only the speed reference is given. It is also referred as run off mode

6.Step (Controller Mode 6):

In this mode the closed loop feedback is made by the PLL-Observer. To ensure, that the PLL-Observer is working properly, the PLL-Observer is executed in parallel to a certain speed. After the observer shows the correct angle and the speed of the rotor, then the output of the observer is fed to the speed controller and dq-Transformation.

For the speed and current controller, the same parameters are used as in the simulation chapter (Table 2.1 and 2.2). The reference value of the d component of the

current is set to zero.

For implementation of the PLL-Observer two controller board is used. The first controller board is made at PES-Laboratory (Figure 5.4). This controller board has a microcontroller with a CPU-clock of 150 MHz and has its Firmware. The current and speed controller structure is implemented in the same interrupt function. An appropriate interrupt frequency for the controller is about 135 kHz without PLL-Observer. However, this interrupt frequency will be not enough to execute the complete code with the observer, because the interrupt execution time is exceeded with the implementation of the PLL-Observer. Therefore, the interrupt frequency is reduced to 65 kHz, while the current and voltage measurements are taken at each second interrupt period from the microcontroller. The timing parameters for the 1.Controller Board are shown in Table 5.3.

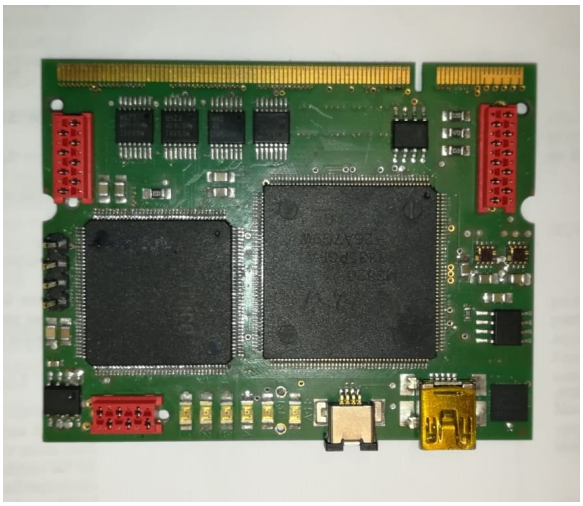

Figure 5.4: 1. Controller Board (PES-Laboratory)

Parameter	Value
t_{int} (μs)	15.8
t_{obs} (μs)	3.159
$t_{controller}$ (μs)	6.42

Table 5.3: The timing parameters for 1.Controller Board

An advantage of this controller board is that it has a FPGA module on the controller board to obtain the register values. This is made with a separate *Hardware Monitor Device* and the register values can be monitored on an oscilloscope directly. Therefore, the results are taken from oscilloscope and plotted in Matlab for this controller board.

An important *problem* for this controller board is the reduced interrupt frequency. With the reducing the interrupt frequency and changing the sampling time of the ADC conversation at each second interrupt period, the required resolution of the current and voltage measurements for high speed range will be reduced and will not satisfy the current controller. Therefore, the experiments with this controller board are made up to 50 *krpm*. The implementation of the code on this controller board is thought as a intermediate step for a new controller board.

Due to insufficient CPU usage of the first controller, the Celeroton AG has designed a new controller board with higher CPU-Clock of 200 MHz (Figure 5.5). This controller board has a microcontroller with two cores. One core is for CPU and another one is CLA (Control Law Accelerator). In case the CPU load is to heavy, some of code can be divided and execute on the CLA part. In this thesis the current and speed controller is implemented in the CLA and the PLL-Observer is implemented in CPU-Core.

Figure 5.5: 2. Controller Board (Celeroton AG)

Parameter	Value
$t_{int,CPU}$ (μs)	7.57
t_{obs} (μs)	1.7
$t_{int,CLA}$ (μs)	7.57
$t_{control}$ (μs)	2.77

Table 5.4: The timing parameters for CPU and CLA

5.1.1 Start-up Strategy

After implementation of all controller mode in the previous section successfully, the speed and position estimations of the PLL-Observer are executed in parallel with the position sensor. However, the PLL-Observer is required to connect to the controller in series to replace the position sensor. To start the machine from zero speed is a difficult challenge [13]. Most of the observer has no ability to start the machine from zero speed. For PLL-Observer the controller gains are exceeded at low speed range, therefore the machine must be accelerated up to a certain speed and the transition from the open loop to the closed loop observer is made in this speed. Without using the down-scaled controller gain parameters, the lowest transition speed is about 10 $krpm$. The transition result for the 2.Type PLL-Observer at 10krpm is shown in Figure 5.6 for one phase current. The phase current drops for a short time, but frequency remains the same. About in 0.2 seconds, the phase current takes its amplitude value and shows stable behave at steady state. The speed response of the observer at transition is shown in Figure 5.7. The drop of the observer speed negligible small. The 1. Type PLL-Observer shows the same results for transition response. Therefore, the transition results for 1.Type PLL-Observer are not shown.

Another start-up strategy is to start the observer at still stand of the motor. The

motor acts like a resistive load and sinusoidal current is enhanced on the terminal of the motor. The transition is made at 50 Hz of phase current and controller gain parameters are down-scaled gain parameters (Figure 5.8 and 5.9). The stabilizing the phase current takes long time and it shows high overshooting with the comparison of previous method. The phase current drops fast to its reference value, but this causes an overshooting on the observer speed. Therefore, for the rest of this report all transitions are made with a running motor .

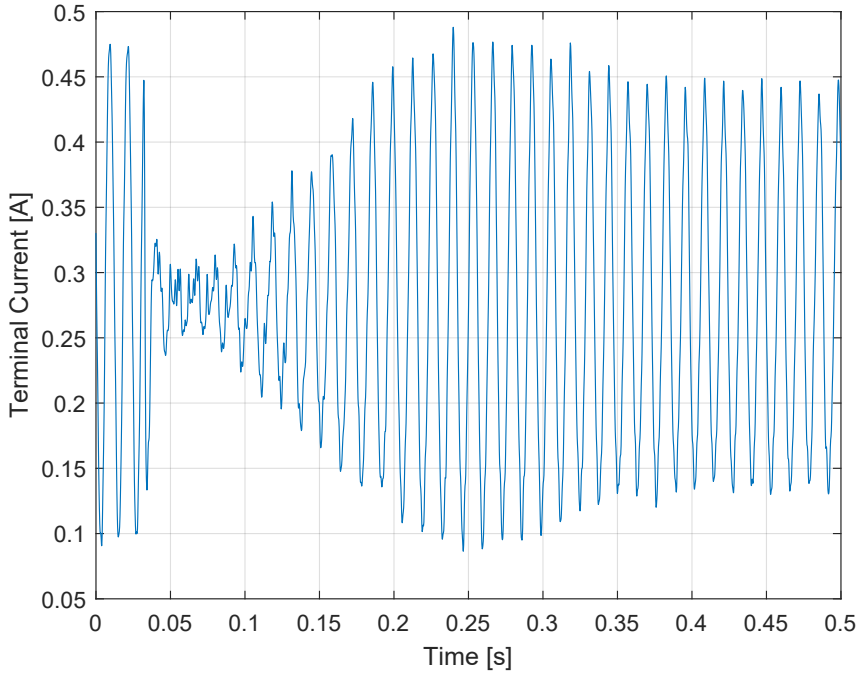

Figure 5.6: One phase current at transition from open loop to closed loop for 2.Type PLL-Observer at 10 $krpm$

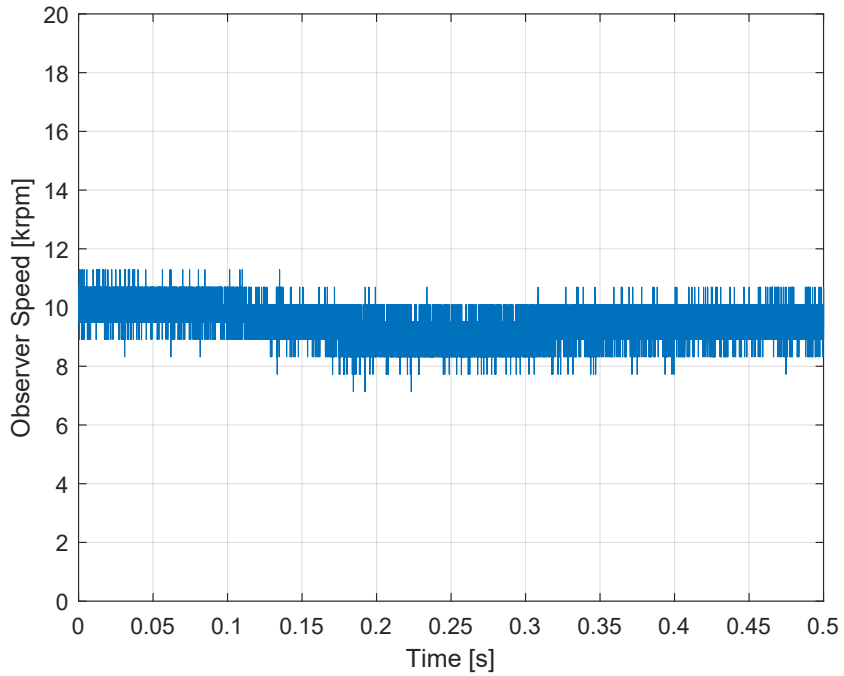

Figure 5.7: Observer speed at transition from open loop to closed loop for 2.Type PLL-Observer at 10 *krpm*

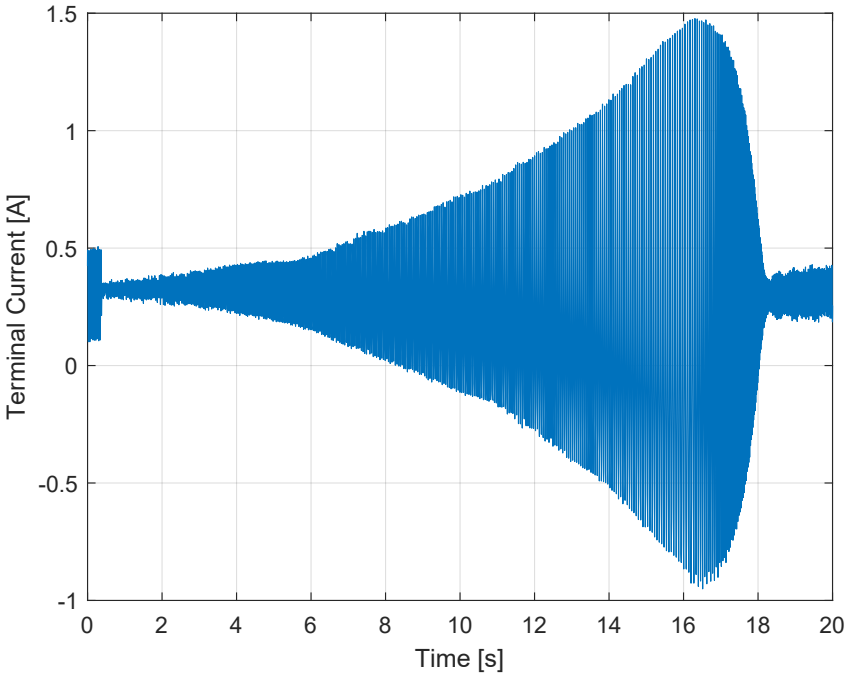

Figure 5.8: Phase current at transition from open loop to closed loop for 2.Type PLL-Observer at 3 *krpm* (50 Hz phase current) at still stand of rotor

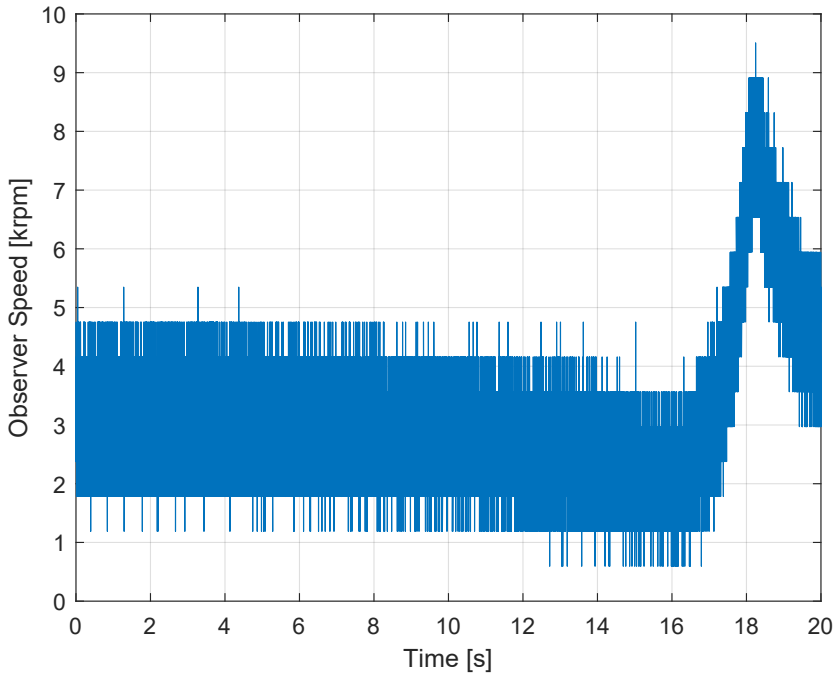

Figure 5.9: Observer speed at transition from open loop to closed loop for 2.Type PLL-Observer at 3 $krpm$ (50 Hz phase current) at still stand of rotor

5.2 Experimental Results

After the open loop transition at 10 $krpm$ is chosen for the start-up strategy, several experiments are made for both type of PLL-Observer. This section is divided into two parts.First part will show the results for the 1.Controller Board experiment results and the second part will show the 2.Controller Board experiment results. In all experiments the position sensor is also runned in parallel to the PLL-Observer. Additionally, the sensor speed is an output of a PI controller, which takes the measured position of the sensor as input.

5.2.1 Experimental Results with 1.Controller Board

First experiments are made with the 1.Controller Board. The highest speed, which is done with the experiments is 50 $krpm$. However, a higher speed is possible up to 120 $krpm$ with the interrupt frequency of 65 kHz. However, above this speed the resolution for current and voltage measurements are insufficient for current controller and PLL-Observer. The experiments with the 1.Controller Board are considered only for a intermediate step for the 2.Controller Board.

First experiments are made with the 1.Type of PLL-Observer with down-scaled controller gain parameters (Figure 5.10). The expected phenomena is seen for this experiment. Namely, the speed of the 1.Type PLL-Observer has a lower accelerating than the speed of the sensor. The reason for this phenomena is that the bandwidth of the observer is reduced according to the speed limit (20 $krpm$). This causes on the speed controller bandwidth a sacrificing in convergence rate at low speed range, which is below the speed limit. After the observer speed has reached the speed limit of the controller gain parameters, the observer speed is able to follow the sensor speed.

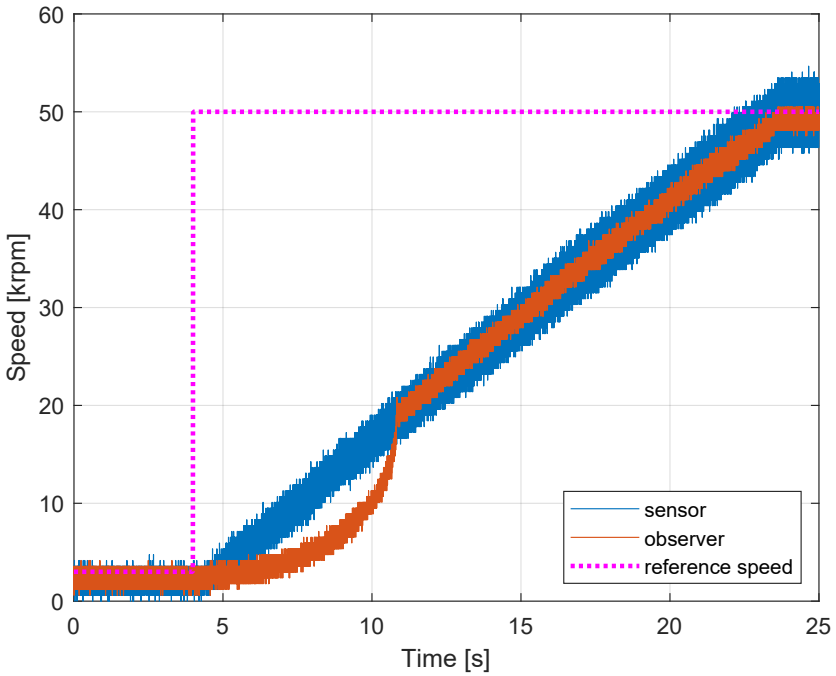

Figure 5.10: Speed step response of 1.Type PLL-Observer with down-scaled controller gain parameters

The same experiment is made for the 2.Type of PLL-Observer (Figure 5.11). It shows the similar phenomena, however the acceleration of the observer speed is slower and jumps to higher speed (30 *krpm*) before the speed limit value is reached. Above 30 *krpm* the 2.Type PLL-Observer can follow the speed of the sensor.

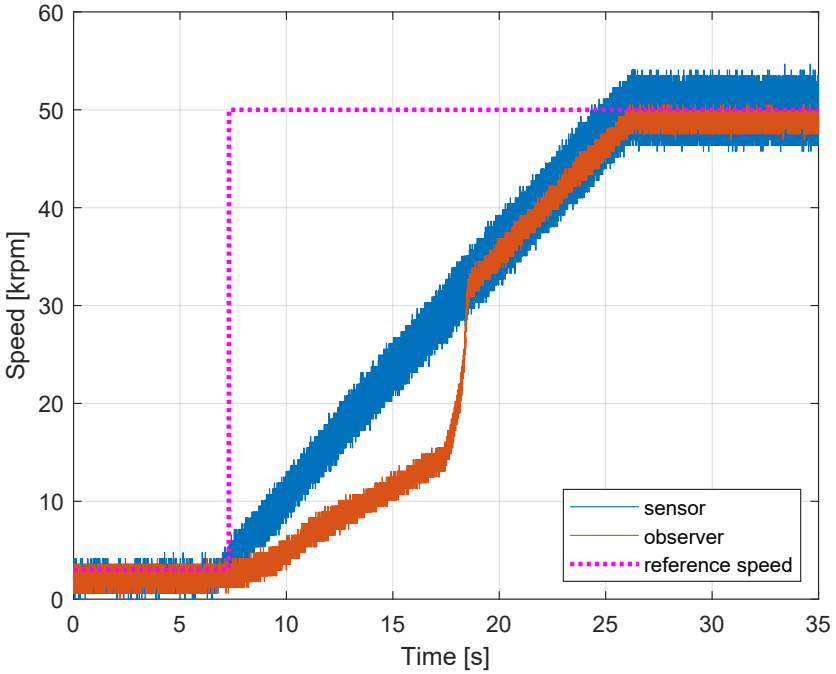

Figure 5.11: Speed step response of 2.Type PLL-Observer with down-scaled controller gain parameters

For the rest of the experiments the down-scaled controller gain parameters is not used anymore. The rest of the experiments are made with the normal controller gain parameters of the PLL-Observer, if nothing else is stated.

Another experiment for the 1.Type PLL-Observer is a step response from 20 *krpm* to 50 *krpm* (Figure 5.12). In this experiment, it is shown that, after the speed is accelerated to 50 *krpm*, the speed shows an offset error about 1 *krpm*. This phenomena was also seen in the simulations. The reason is that the speed of the observer is the output of the I-Controller and P-Controller, which reduces the offset error, is not used. The speed error is getting higher with the acceleration, because the speed of the sensor shows high variation and speed error is calculated between the difference of the sensor speed and observer speed (Figure 5.13). Therefore, the speed error is shown in this report, but is not a good reference for accuracy of the observer speed. However, the position error, which is the difference of the position of sensor and observer is a important reference for accuracy of the observer position and this smaller than 0.2 *rad*, which is a good result (Figure 5.14).

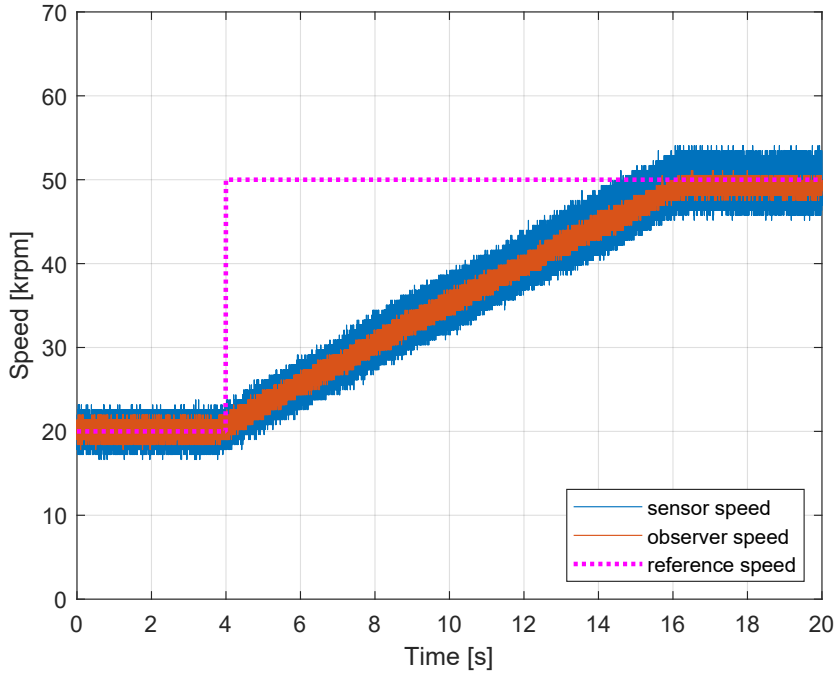

Figure 5.12: Speed step response of 1.Type PLL-Observer

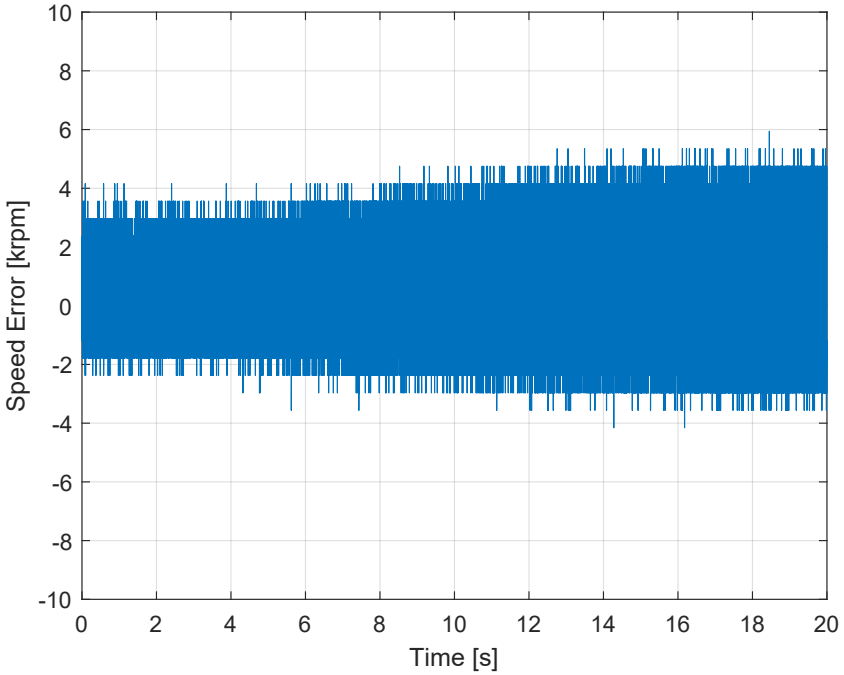

Figure 5.13: Speed error for speed step response of 1.Type PLL-Observer

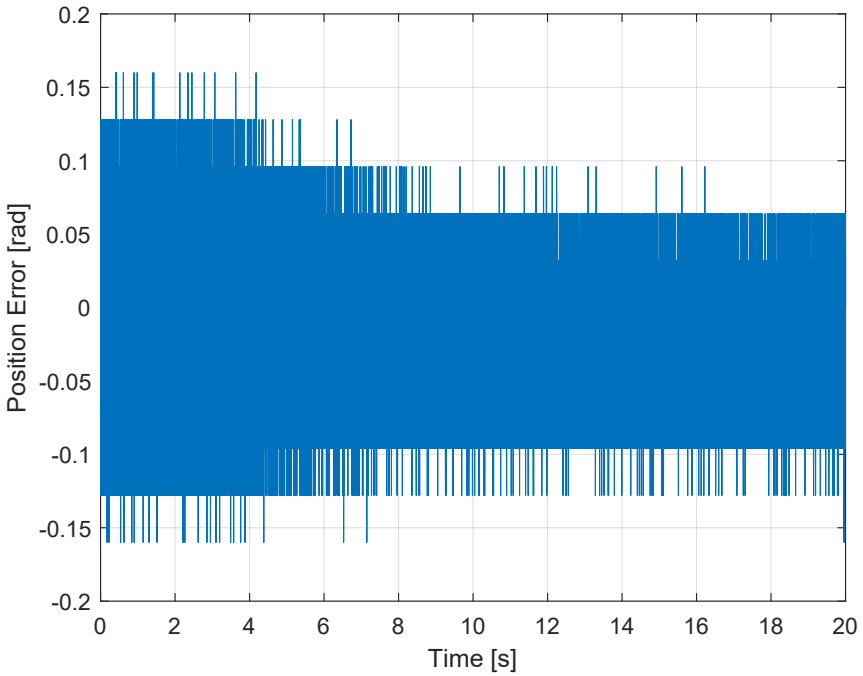

Figure 5.14: Position error for speed step response of 1.Type PLL-Observer

The same step response experiment is made with the 2.Type PLL-Observer. It shows very similar behave to the 1.Type PLL-Observer and the same interpretation is valid as 1.Type PLL-Observer. It must be noted that this behave is not seen in the simulations. Which means that, the speed of the observer is under the reference value of speed. Therefore, it shows an offset value difference from reference value at steady state. This was not seen in the simulation. Only difference between the simulation and this experiments are the reference speed, which is for simulation 350 *krpm* and for this experiment 50 *krpm*. The reason for this phenomena is not clear.

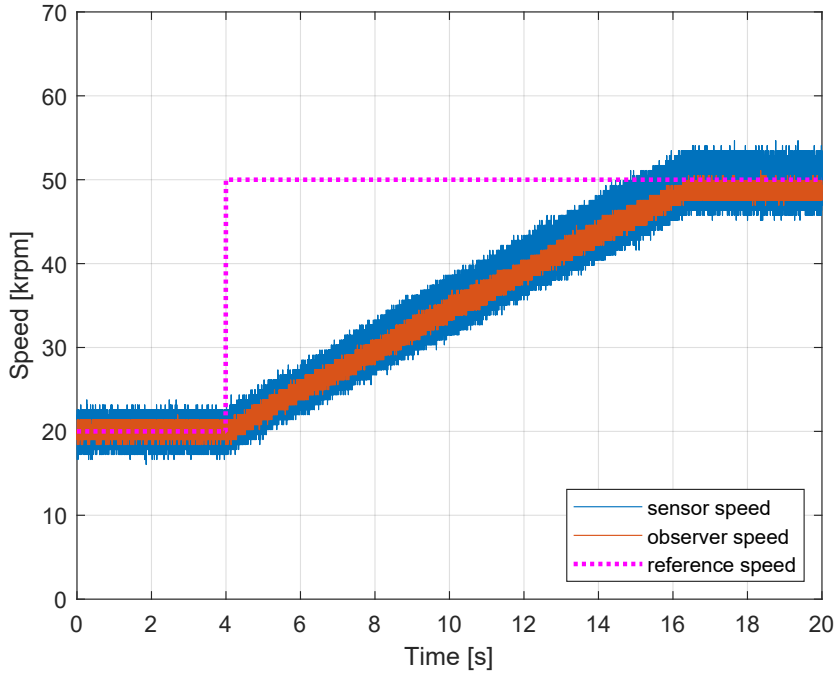

Figure 5.15: Speed step response of 2.Type PLL-Observer

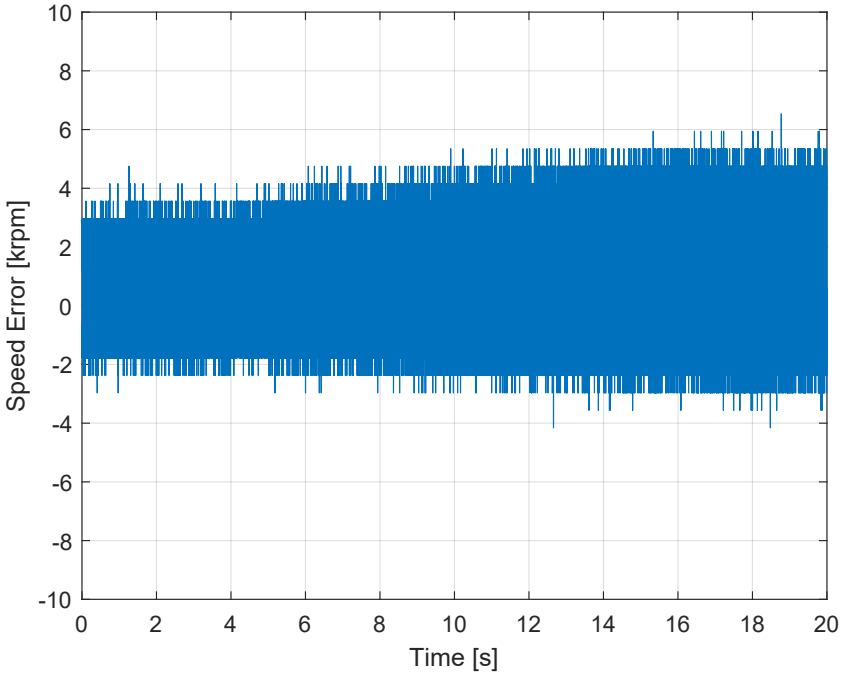

Figure 5.16: Speed error of speed step response of 2.Type PLL-Observer

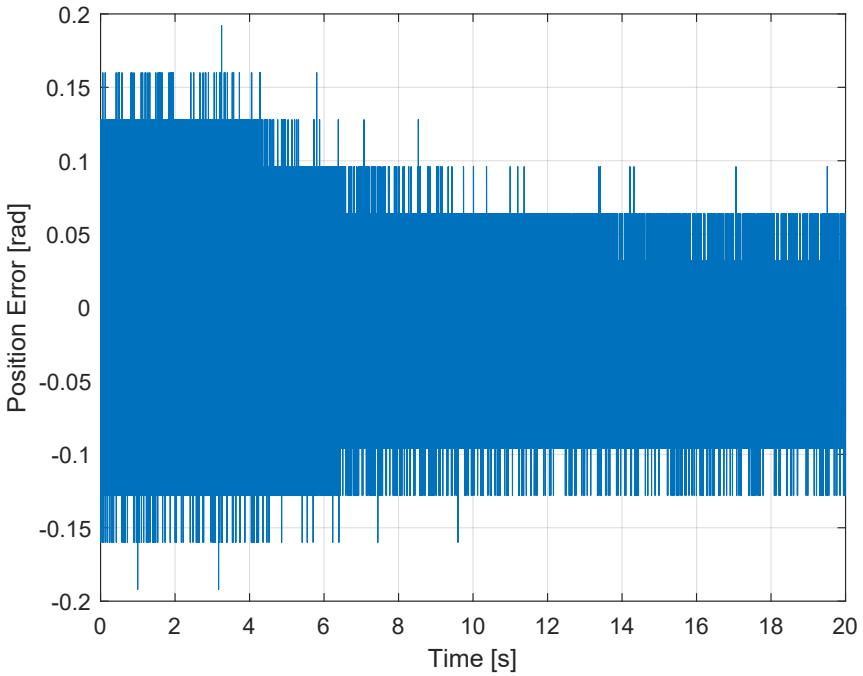

Figure 5.17: Position error of speed step response of 2.Type PLL-Observer

The experiments with the 1.Controller Board is finished and any further experiments are not made, because the controller board will be replaced with a new one due to the low interrupt frequency of the 1.Controller Board. The rest of experiments with step response and load response are made with the 2.Controller Board. It must be noted that, the measurement in this section are made on oscilloscope with the Hardware Monitor Device. For the 2.Controller the measurements are made with the software of Celeroton AG. Therefore, the measurements with the 1.Controller Board show more noises than the 2.Controller Board measurements.

5.2.2 Experimental Results with 2. Controller Board

The same controller modes are implemented for the 2. Controller Board. With this controller board, it is expected to reach the nominal speed and nominal torque of the B2B-Motor. Therefore the experiments with the 2.Controller Board are made. The interrupt frequency is set to 135 kHz for CLA and CPU. The current and speed controller are implemented on the CLA and the both PLL-Observer Types are implemented on the CPU. The CLA is configured from CPU and with the first ADC measurements the interrupt function of CLA is started. The experiments for 2. Controller Board are only made with the controller gain parameters of the PLL-Observer, which is not down-scaled (Eq. 4.4).
The first experiment is made for the transition response at 10 $krpm$ for the 1.Type PLL-Observer (Figure 5.18). In general, the speed of the observer drops about 1 $krpm$ and after 1 sec it comes up to the reference value, however it shows high variations during transition. The reason for this phenomena is the controller gain parameters is not down-scaled and it is under the speed limit of the PLL-Observer. Therefore the dynamic of the 1.Type PLL-Observer is poor to reduce the high variation. The position of observer and position error are shown in Figure 5.20 and 5.21. The error of the position is smaller than 0.2 rad, which is a satisfied result.

The Figure 5.19 shows the speed error. The speed error shows high error about 10 *krpm* at the beginning of transition. However, the speed error varies between 2 *krpm* and -2 *krpm* at steady state.

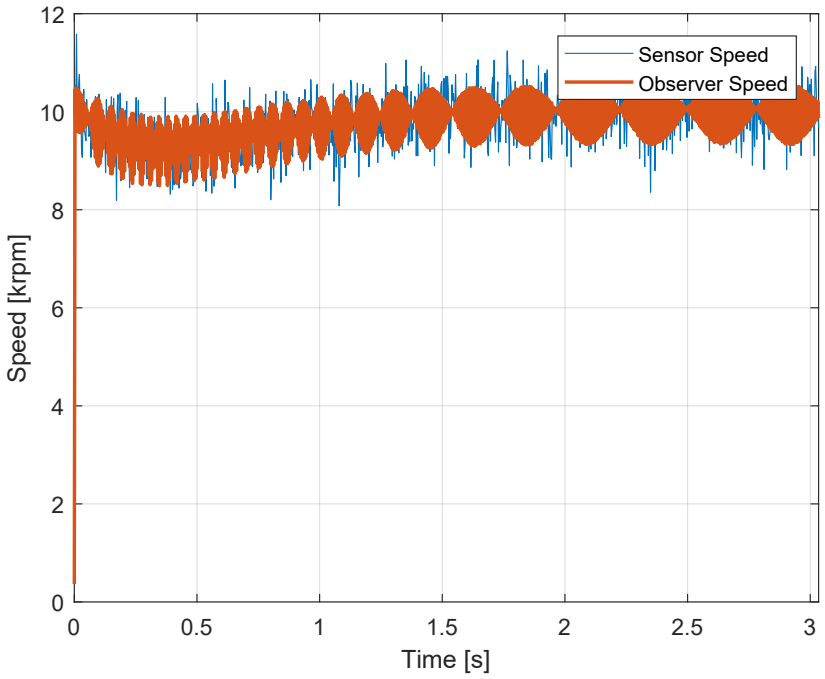

Figure 5.18: Speed transition at 10 krpm from open loop to closed loop observer for 2.Controller Board without load-1.Type PLL

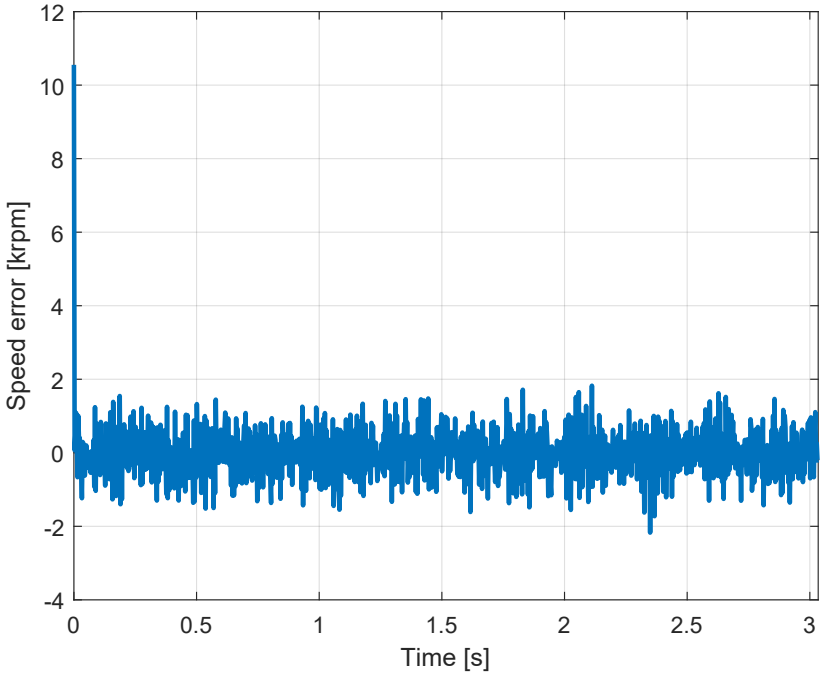

Figure 5.19: Speed error transition at 10 krpm from open loop to closed loop observer for 2.Controller Board without load - 1.Type PLL

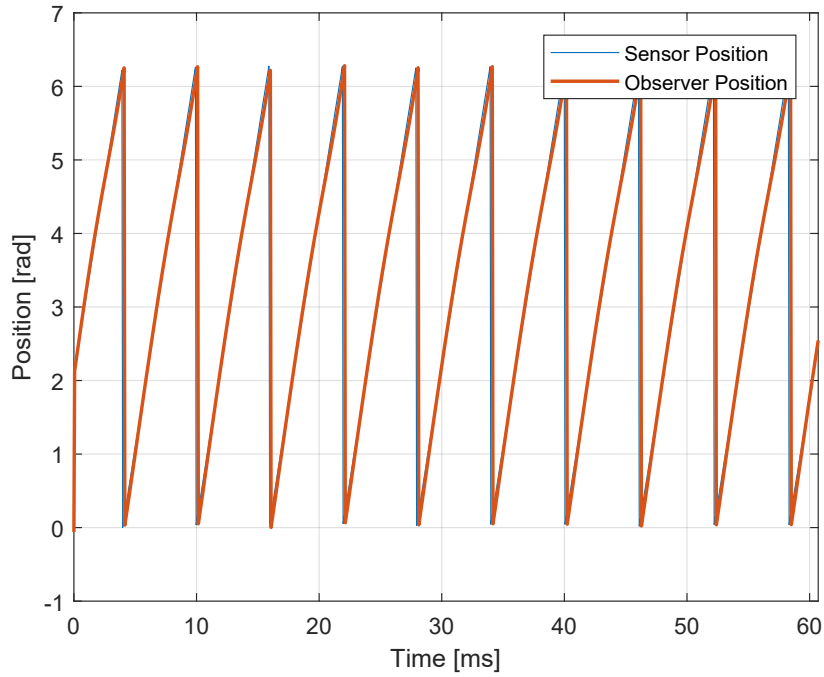

Figure 5.20: Position transition at 10 krpm from open loop to closed loop observer for 2.Controller Board without load - 1.Type PLL

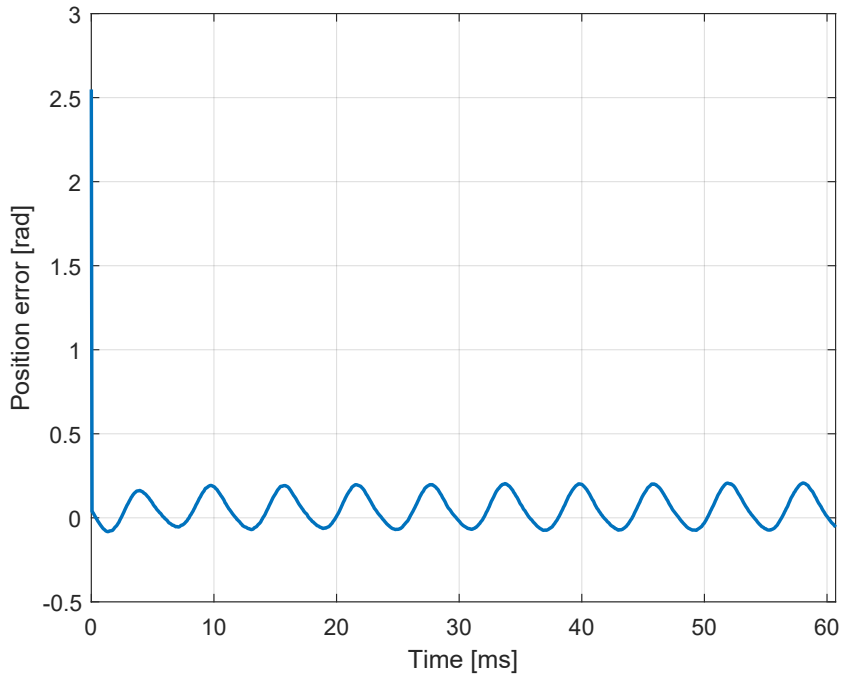

Figure 5.21: Position error transition at 10 krpm from open loop to closed loop observer for 2.Controller Board without load - 1.Type PLL

The next experiment is made for the transition response at 10 *krpm* for the 2.Type PLL-Observer (Figure 5.22). The observer speed drops again about 1 *krpm* and the observer speed comes up to the reference speed about in 1.5 *sec*. However, the high variation of the observer speed, which occurs for the 1.Type PLL-Observer, is significantly reduced. The reason for this phenomena is the 2.Type PLL-Observer shows higher dynamic than the 1.Type PLL-Observer. The position of the observer with sensor position and the position error is shown in Figure 5.24 and 5.25. The position error of the 2.Type PLL-Observer is higher then 1.Type PLL-Observer. Because at low speed range, the 2.Type PLL-Observer shows high overshooting. The figure 5.23 shows the speed error. The speed error shows high error about 8 *krpm* at the beginning of transition. However, the speed error varies between 1.5 *krpm* and -1.5 *krpm* at steady state. The speed error of the 2. Type PLL-Observer is lower than the 1. Type PLL-Observer.

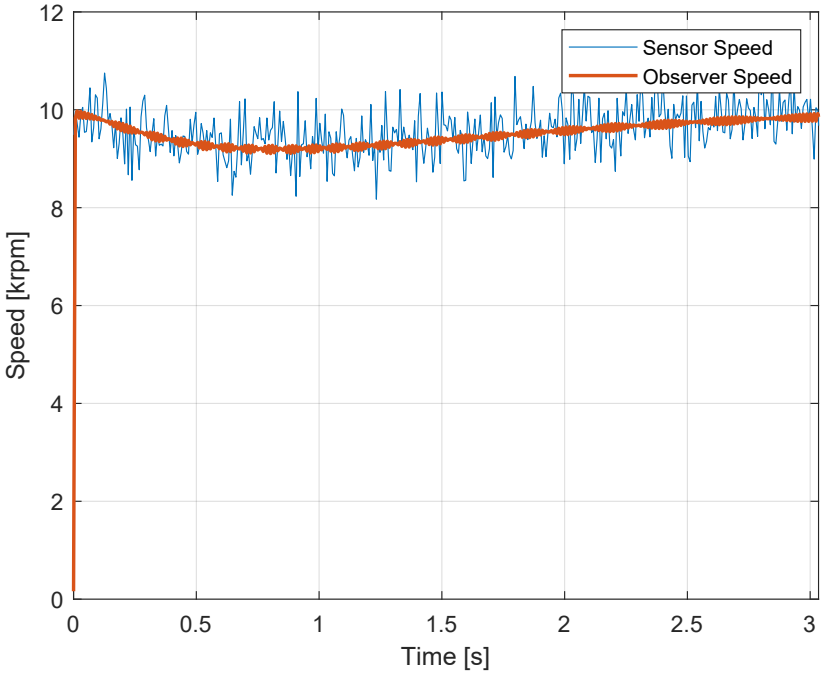

Figure 5.22: Speed transition at 10 krpm from open loop to closed loop observer for 2.Controller Board without load-2.Type PLL

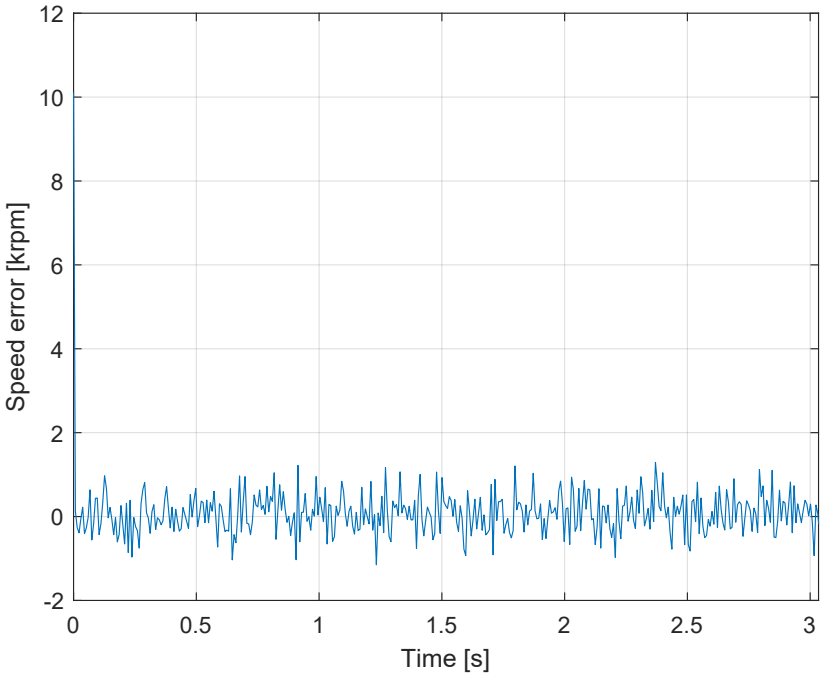

Figure 5.23: Speed error transition at 10 krpm from open loop to closed loop observer for 2.Controller Board without load - 2.Type PLL

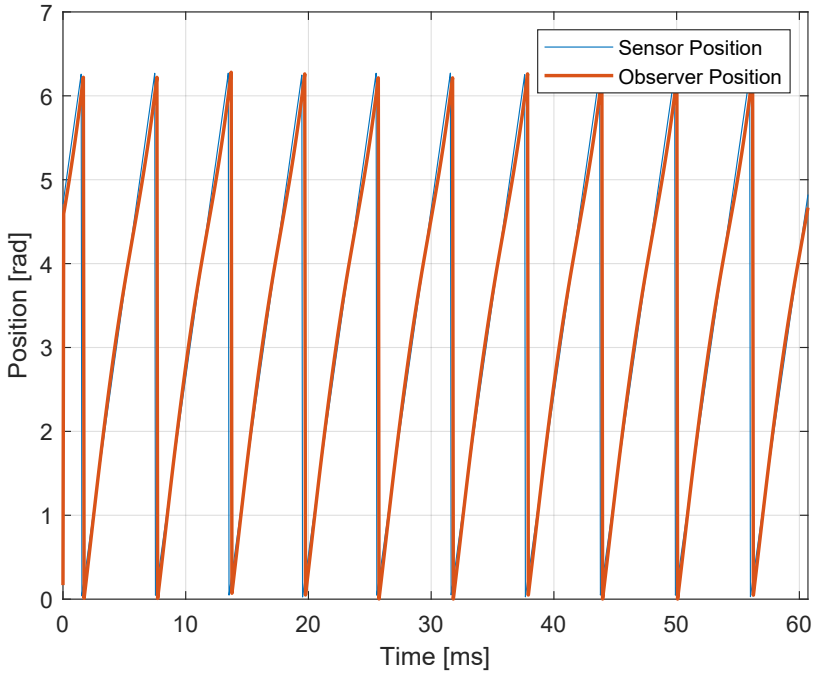

Figure 5.24: Position transition at 10 krpm from open loop to closed loop observer for 2.Controller Board without load - 2.Type PLL

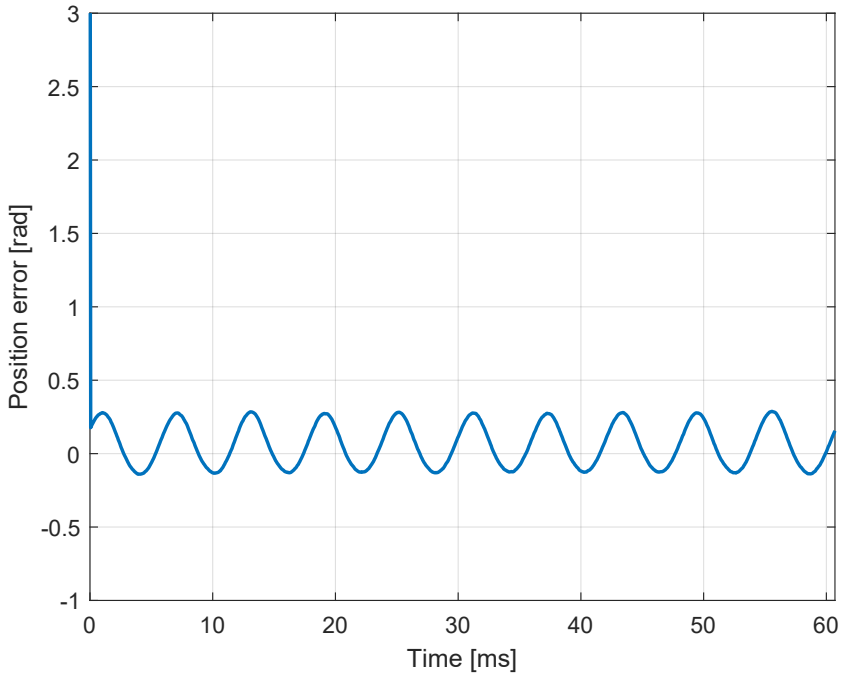

Figure 5.25: Position error transition at 10 krpm from open loop to closed loop observer for 2.Controller Board without load - 2.Type PLL

A step response experiment is made for the 2.Type PLL-Observer with the 2.Controller Board (Figure 5.26). The high variations at low speed (10 *krpm*) range is reduced at 50 *krpm*. However, it shows a overshoot about 1 *krpm*. The position error is not changed to much during the step response (Figure 5.28). The figure 5.27 shows the speed error. The speed error varies between 1.5 *krpm* and -1.5 *krpm* at steady state. The at the end of the speed response the speed error is reduces about 0.5 *krpm*.

During the experiments with the 1.Type PLL-Observer a problem has occurred . The problem is that, when the observer speed is higher than 70 *krpm* the observer speed acts unstable. The reason for unstable behave for the 1.Type PLL-Observer is not found. Any further experiments is not made for 1.Type PLL-Observer and more time is investigated for the 2.Type PLL-Observer.

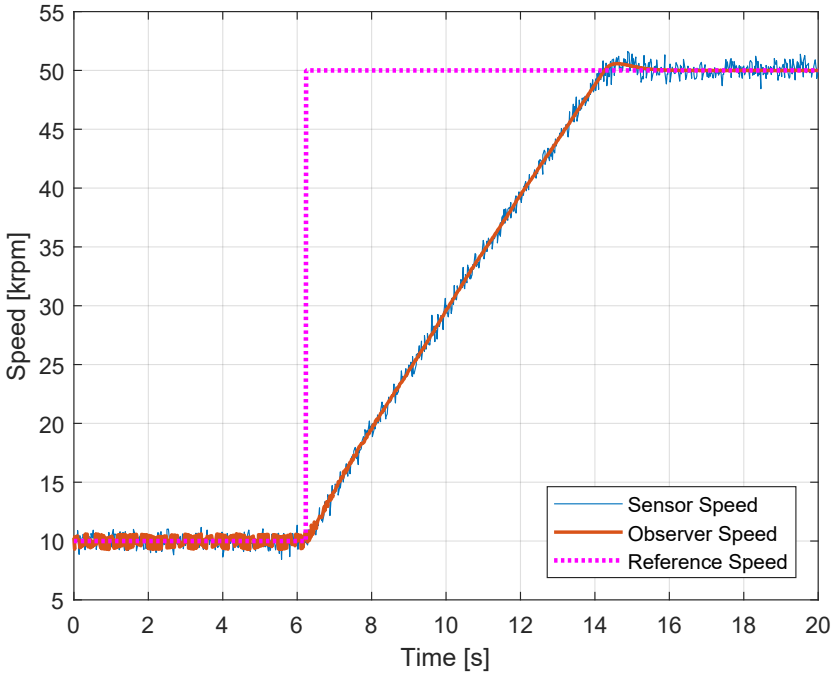

Figure 5.26: Speed step response from 10 *krpm* to 50 *krpm* for 2.Controller Board without load - 1.Type PLL

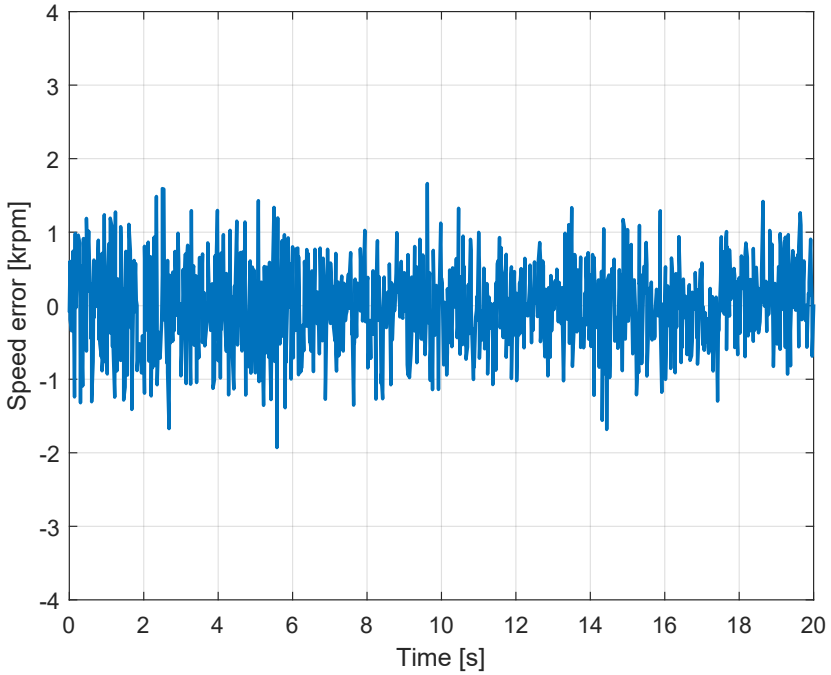

Figure 5.27: Speed error while speed step response from 10 *krpm* to 50 *krpm* for 2.Controller Board without load - 1.Type PLL

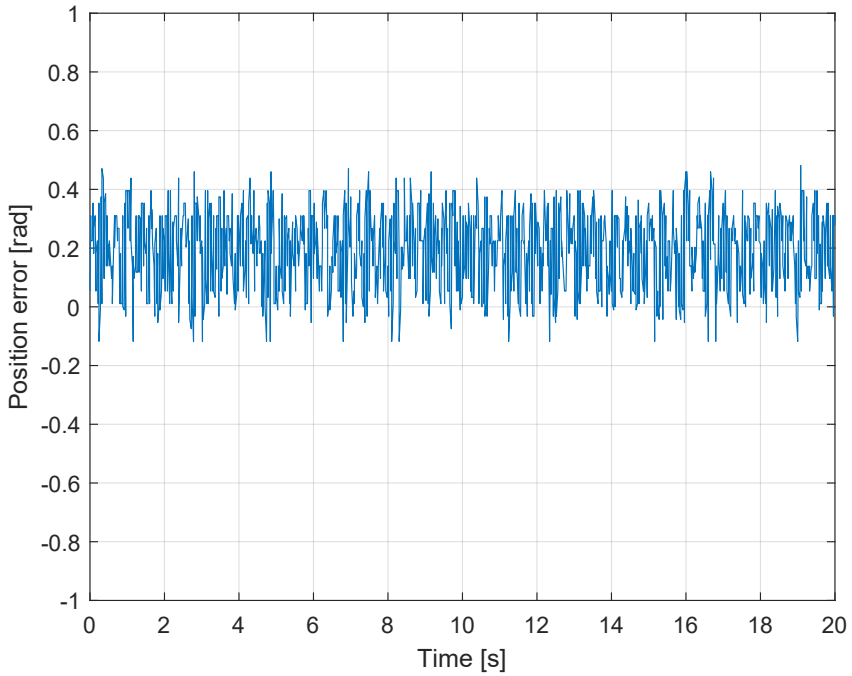

Figure 5.28: Position error while speed step response from 10 *krpm* to 50 *krpm* for 2.Controller Board without load - 1.Type PLL

The step response experiment is tried for nominal speed of the motor. Unfortunately, the B2B motor is not capable to run above the 200 *krpm*. It comes out, that B2B machine has two prototype and one prototype has a nominal speed about 200 *krpm*. Although, the another prototype has a nominal speed of 350 *krpm*, it was not available to test it due to absent. A second problem with the B2B motor, which has a nominal speed of 200 *krpm*, is that, it is occurred an unexpected noises above the speed of 170 *krpm*. Therefore, to safe the electronic part and motor itself, the highest speed is limited to 170 *krpm*. In Figure 5.29, the step response from 10 *krpm* to 170 *krpm* is shown. The speed acceleration to 170 *krpm* is reached successfully. The figure 5.30 shows the speed error for the step response. During the speed acceleration of the motor, the speed error becomes higher, because the speed of the sensor varies higher at the speed of 170 *krpm*. The position error of the 2.Type PLL-Observer is reduced to close to zero (Figure 5.31). The performance of the 2.Type PLL-Observer up to 170 *krpm* without load is gorgeous.

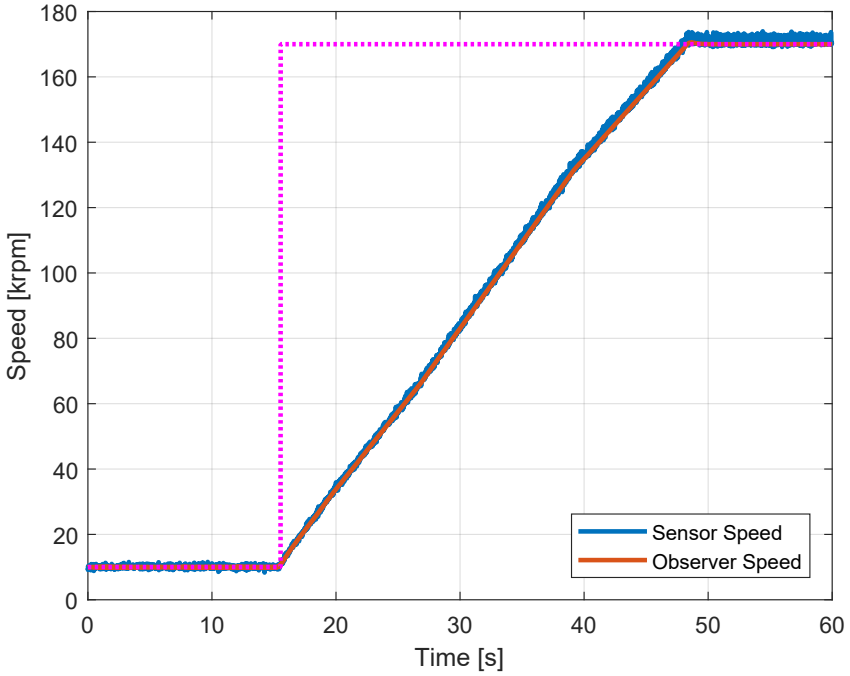

Figure 5.29: Speed step response from 10 *krpm* to 170 *krpm* for 2.Controller Board without load - 2.Type PLL

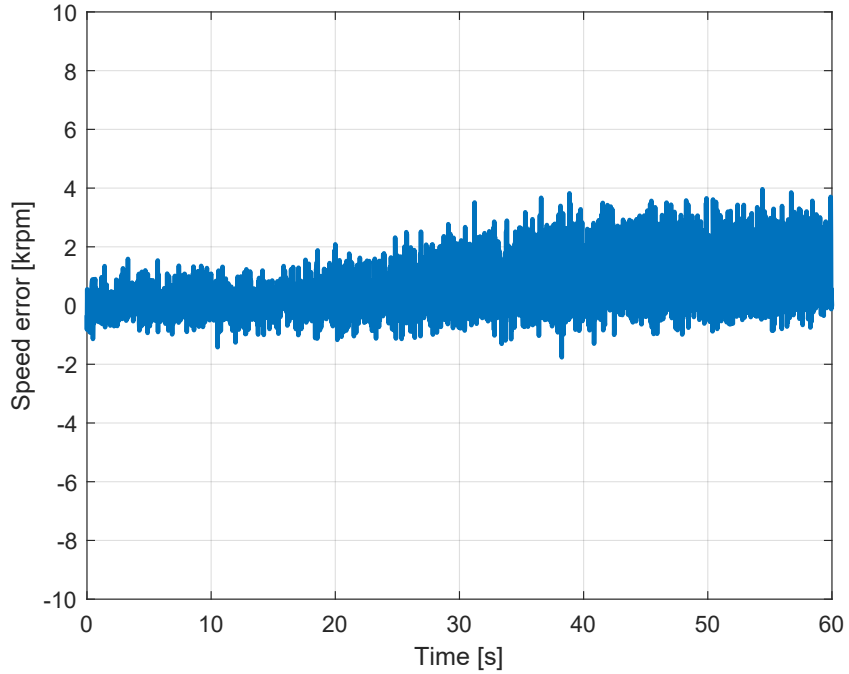

Figure 5.30: Speed error while speed step response from 10 *krpm* to 170 *krpm* for 2.Controller Board without load - 2.Type PLL

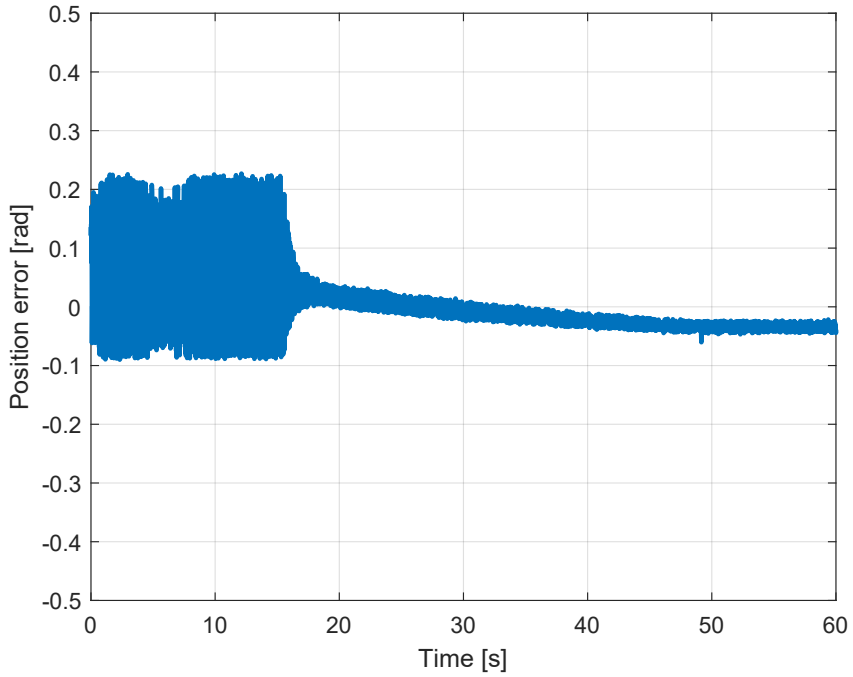

Figure 5.31: Position error while speed step response from 10 *krpm* to 170 *krpm* for 2.Controller Board without load - 2.Type PLL

Another important research about this project is to know the load response of the PLL-Observer. The load response for the observer is made only for 2.Type PLL-Observer due to time restriction. To made an experiment of load torque an internal Celeroton inverter is used (CC-75-500). While one side of the Motor is connected to the VSI Inverter, the other side of the motor is connected to the CC-75-500-Inverter. The machine is accelerated up to 150 krpm with the VSI-Inverter 5.33. At this speed the CC75-500-Inverter is also set to 150 krpm. The speed of the machine has been tried to reduce with the CC-75-500-Inverter. The power flow is ensured from the VSI-Inverter to CC-75-500 to safe the VSI-Inverter. With the reducing the speed on the CC-75-500-Inverter the output power of the CC-75-500-Inverter is measured. The output power is reduced step by step up to -80 $Watt$ (Figure 5.32). At this output power, the highest phase current for the CC-75-500 is almost reached and the experiment is stopped. The speed of the observer shows very small deviation. To better determine the accuracy of the speed error, it is included a speed error regarding to reference speed in Figure 5.34. Both the speed error and the position error is negligible small (Figure 5.35).

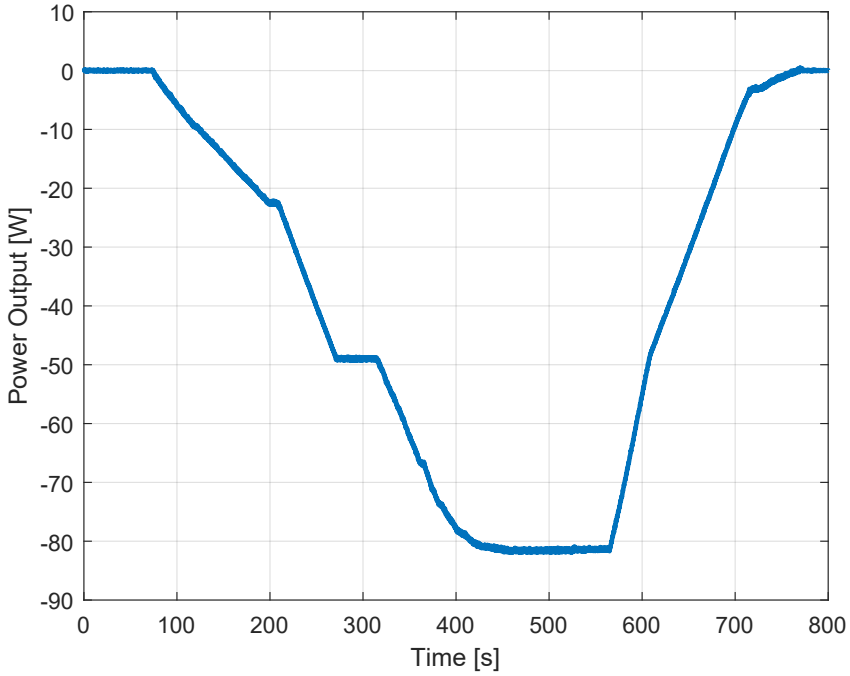

Figure 5.32: Output power of inverter of Celeroton - 2.Type PLL

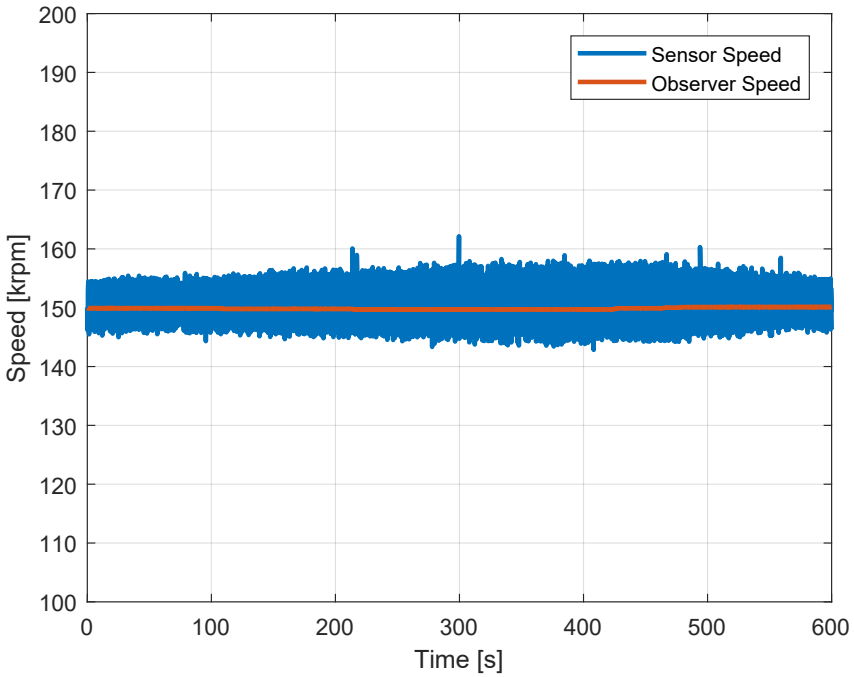

Figure 5.33: Load response at 150 *krpm* from 0 *W* to 80 *W* for 2.Controller Board without load - 2.Type PLL

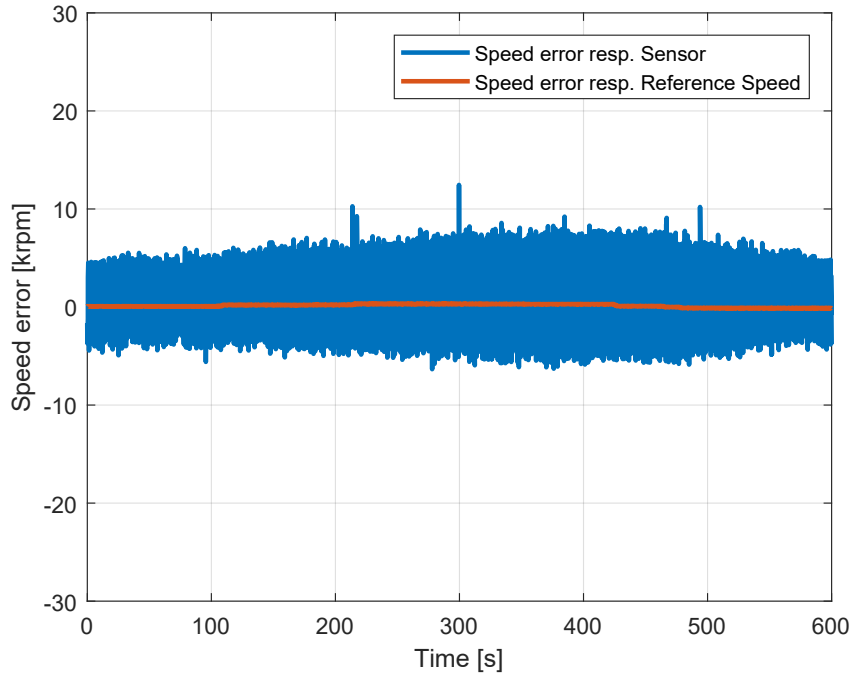

Figure 5.34: Speed error while load response at 150 *krpm* from 0 *W* to 80 *W* for 2.Controller Board without load - 2.Type PLL

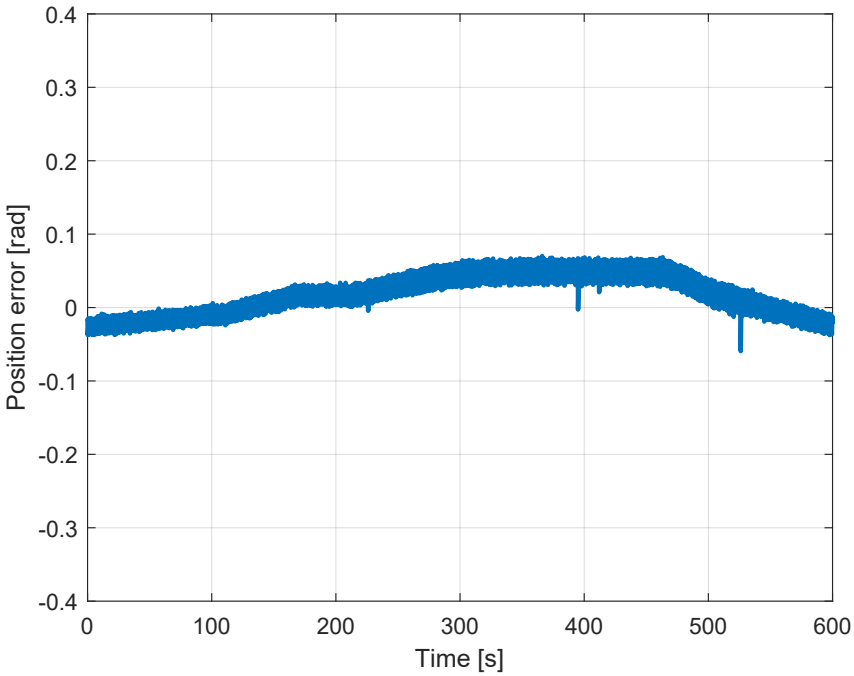

Figure 5.35: Position error while load response at 150 *krpm* from 0 *W* to 80 *W* for 2.Controller Board without load - 2.Type PLL

Finally, the phase currents at speed of 170 *krpm* without load is shown in the Figure 5.36 at the steady state. The phase currents is still far away from rated phase currents. However at speed of 150 *krpm* the phase current is near to the rated phase current of the inverter (Figure 5.37). Therefore, increasing the output power to much for load will not possible without water cooling.

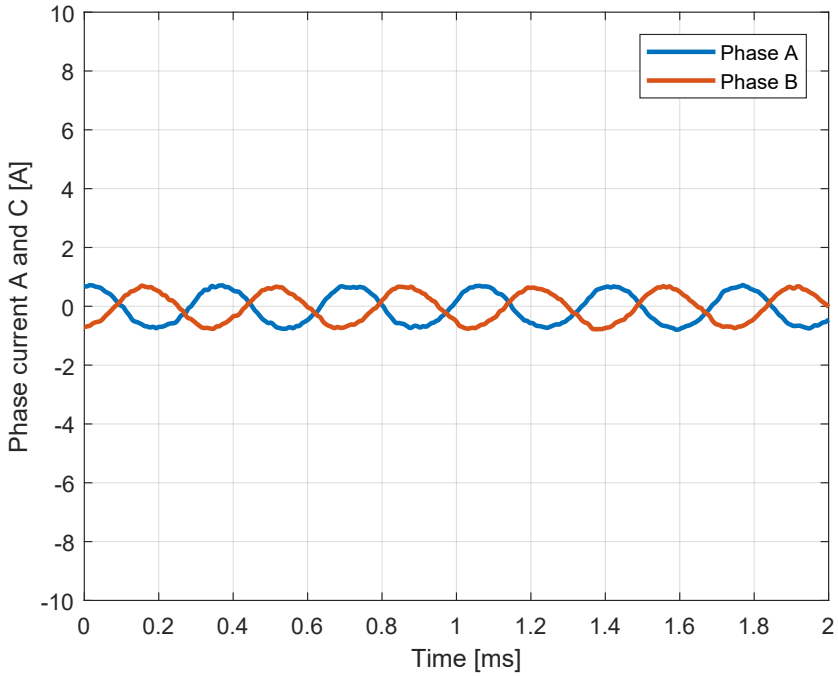

Figure 5.36: Phase Current A and C at 170 *krpm* without load with 2.Controller Board- 2.Type PLL

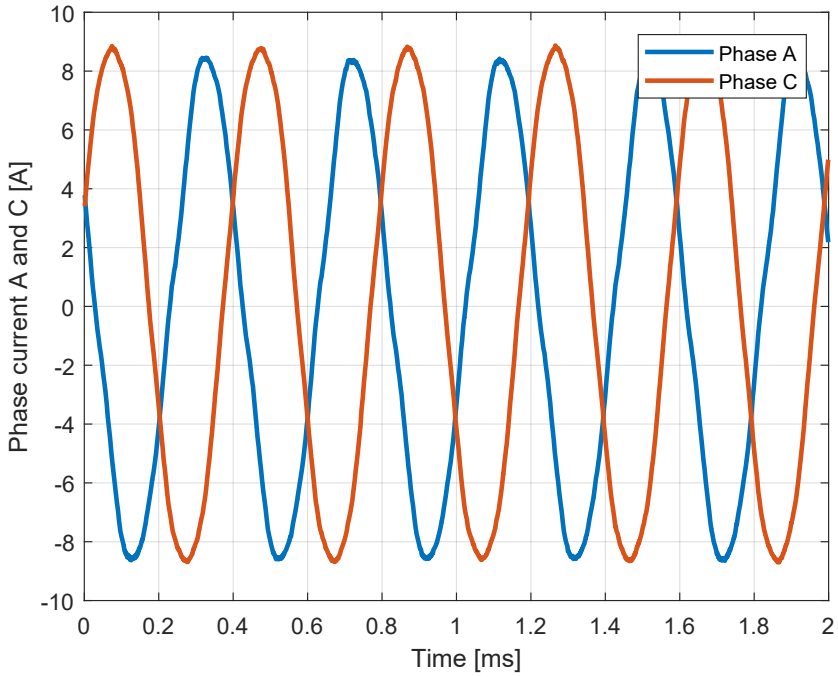

Figure 5.37: Phase Current A and C at 150 *krpm* with load of 80 *W* with 2.Controller Board- 2.Type PLL

Chapter 6

Conclusion

6.1 Summary

At the end of this master thesis, a working PLL-Observer is designed up to 170 *krpm* without load and 150 *krpm* with load.

With using the values of phase currents and voltages of the VSI and parameters of B2B , the both type of the PLL-Observer are implemented on two different controller Board. In the 1. Controller board, a CPU execution time problem has occurred. To overcome this problem the interrupt frequency is reduced, however this has brought another problem, which has reduced resolution of measurements for high speed range. Therefore, the controller board is changed with a new one, which has a higher clock frequency and two cores. The entire controller code is implemented on CLA-core and the PLL-Observer code is implemented on CPU-core. The execution time for controller and observer is reduced significantly.

The 1. Type PLL-Observer is modeled in MATLAB-Simulink and a stable system is verified up to 350 *krpm*. However, the 1. Type PLL-Observer has showed a stable working point without load between 3 *krpm* and 70 *krpm* in the hardware experiments. A higher speed response is not possible. Increasing the observer speed to higher value, the 1. Type PLL-Observer behaves unstable. In case for an unstable situation, a code is written on DSP, hence the hardware stops immediately for safe the experimental setup. The reason for unstable behavior of 1. Type PLL-Observer is not determined yet. Due to time restriction, an examination of the problem of 1. Type PLL-Observer was not possible.

The same steps are made for the 2. Type PLL-Observer. A verification in simulation for a stable system is made up to 350 *krpm*. In the Hardware experiments, the used motor cannot be operated above 170 *krpm*. The reason for that is, above this 170 *krpm*, it occurs in the B2B-machine noises and after 200 *krpm* the machine losses its speed. It comes up the used prototype of B2B-Machine has a nominal speed of 200 *krpm*. Above 170 *krpm* B2B-machine begins to make noises.

Therefore, the speed during the experiments is limited to 170 *krpm* for safe the electronics. A load response experiment is made for the 2. Type PLL-Observer. The load experiment is made with trying to reduce the speed of the B2B motor with an intern inverter of Celeroton at 150 *krpm*. The load is increased step by step up to 80 W. This value is the almost the limit for this kind of experiment, because the phase current of the intern inverter has reached almost its limit. At

the end of this experiment it is seen that, the 2. Type PLL-Observer is able to behave stable against load response. Within the project of collaboration of PES and Celeroton AG, an observer for the motor prototype of the system (B2B) is successfully implemented at the end of this thesis.

6.2 Outlook

In this some important tasks and possible improvements are given for further development for this project:

1.Testing the 2. Type PLL-Observer with another prototype of B2B-Machine with nominal speed of 350 krpm: The 2. PLL-Observer is not tested up to nominal speed 350 $krpm$ and nominal power of 500 $Watt$, due to wrong prototype of the B2B-Machine. Therefore, this task must be made with another B2B-Machine, which has a nominal speed of 350 $krpm$

2.Troubleshooting for 1. Type PLL-Observer: The problem for with 1. Type PLL-Observer is not solved, due to time restriction. Its speed operating range is between 3 $krpm$ and 70 $krpm$

3.Testing both type PLL-Observer with new Y-Inverter: PES-Laboratory has designed an another prototype of inverter for the B2B-Machine with the Y-Inverter topology. The rated power of this prototype Y-inverter is 3 times bigger than of the prototype of VSI. The both type of PLL-Observer can be tried on this inverter.

4.Model Reference Adaptive System observer: An advantage of this observer type is that, it reduces the error quantity at low speed range with a reference model. This feature is not present on PLL-Observer.

Bibliography

[1] Jesus de Leon Morales Alain Glumineau. *Sensorless AC Electric Motor Control".* 2014.

[2] J. W. Kolar. *Lecture Material "Power Electronic Systems II".* 2010.

[3] Stulz. *Lecture Material "Antriebssysteme 1 Teil3".* 2017.

[4] A. Piippo and J. Luomi. Adaptive observer combined with hf signal injection for sensorless control of pmsm drives. In *IEEE International Conference on Electric Machines and Drives, 2005.*, pages 674–681, May 2005. doi: 10.1109/IEMDC.2005.195796.

[5] Gheorghe-Daniel Andreescu. Position and speed sensorless control of pmsm drives based on adaptive observer. 09 1999.

[6] J. Xu, B. Xu, W. Ji, G. Shi, and S. Ding. Research on speed sensorless operation of pmsm based on improved mras. In *2017 11th Asian Control Conference (ASCC)*, pages 1423–1427, Dec 2017. doi: 10.1109/ASCC.2017.8287381.

[7] A. Piippo, M. Hinkkanen, and J. Luomi. Adaptation of motor parameters in sensorless pmsm drives. *IEEE Transactions on Industry Applications*, 45(1): 203–212, Jan 2009. ISSN 0093-9994. doi: 10.1109/TIA.2008.2009614.

[8] Zhang Yong Cheng, Xu-Feng. Sensorless control of permanent magnet synchronous motors and ekf parameter tuning research. 2016.

[9] Matti Eskola. *Speed and Position Sensorless Control of Permanent Magnet Synchrounus Motors in Matrix Converter and Voltage Source Converter Applications.* Doctora thesis, Tampere Univercity of Technologie, 2006.

[10] Peter Bader. Celeroton-intern dokumentation pwmdrv/observer.

[11] L. Harnefors and H. . Nee. A general algorithm for speed and position estimation of ac motors. *IEEE Transactions on Industrial Electronics*, 47(1):77–83, Feb 2000. ISSN 0278-0046. doi: 10.1109/41.824128.

[12] Bosshard Roman. *Parameter Estimation and Sensorless Control of an Ultra-High-Speed Permanent-Magnet Synchronous Machine.* Master thesis, Swiss Federal Institute of Technology (ETH) Zurich, 2011.

[13] A. Borisavljevic, H. Polinder, and J. A. Ferreira. Realization of the i/f control method for a high-speed permanent magnet motor. In *The XIX International Conference on Electrical Machines - ICEM 2010*, pages 1–6, Sept 2010. doi: 10.1109/ICELMACH.2010.5607892.

Appendix A

Contents of the Enclosed CD-ROM

- **Administration:** Documents for Administration .
- **Datasheets:** Datasheets of TI-Microcontroller .
- **Literature:** All publications cited in this thesis.
- **Measurements:** Raw measurement data from the experiments.
- **Presentation:** Midterm and final presentation of this thesis.
- **Report:** Latex source of this document.
- **Simulations:** All used simulations.

Eidgenössische Technische Hochschule Zürich
Swiss Federal Institute of Technology Zurich

Declaration of originality

The signed declaration of originality is a component of every semester paper, Bachelor's thesis, Master's thesis and any other degree paper undertaken during the course of studies, including the respective electronic versions.

Lecturers may also require a declaration of originality for other written papers compiled for their courses.

I hereby confirm that I am the sole author of the written work here enclosed and that I have compiled it in my own words. Parts excepted are corrections of form and content by the supervisor.

Title of work (in block letters):

HIGH-SPEED SENSORLESS MOTOR CONTROL WITH IMPROVED POWER ELECTRONICS TOPOLOGIES

Authored by (in block letters):

For papers written by groups the names of all authors are required.

Name(s):	**First name(s):**
ISMAIL	TEZOL

With my signature I confirm that

- I have committed none of the forms of plagiarism described in the 'Citation etiquette' information sheet.
- I have documented all methods, data and processes truthfully.
- I have not manipulated any data.
- I have mentioned all persons who were significant facilitators of the work.

I am aware that the work may be screened electronically for plagiarism.

Place, date	**Signature(s)**
24.08.2018	

For papers written by groups the names of all authors are required. Their signatures collectively guarantee the entire content of the written paper.